Multimodality Imaging of Liver Infections: Differential Diagnosis and Potential Pitfalls[1]

Pablo Bächler, MD
María José Baladron, MD
Christine Menias, MD
Ignacio Beddings, MD
Ron Loch, MD
Eugenio Zalaquett, MD
Matías Vargas, MD
Sarah Connolly, MD
Sanjeev Bhalla, MD
Álvaro Huete, MD

Imaging plays an important role in the diagnosis, characterization, and management of infectious liver disease. In clinical practice, the main contributions of imaging are in detecting early disease, excluding other entities with a similar presentation, establishing a definitive diagnosis when classic findings are present, and guiding appropriate antimicrobial, interventional, or surgical treatment. The most common imaging features of bacterial, viral, parasitic, and fungal hepatic infections are described, and key imaging and clinical manifestations are reviewed that may be useful to narrow the differential diagnosis and avoid pitfalls in image interpretation. Ultrasonography (US), computed tomography (CT), and magnetic resonance imaging allow accurate detection of most hepatic infections and, in some circumstances, may provide specific signs to identify the underlying pathogen and exclude other entities with similar imaging features. In bacterial and parasitic infections, specific imaging features may be enough to exclude a neoplasm and, occasionally, to identify the underlying infectious agent. US and CT are important means to guide percutaneous aspiration or drainage when needed. In viral infections, imaging is critical to exclude entities that may manifest with similar clinical and laboratory findings. Disseminated fungal infections require early detection at imaging because they can be fatal if not promptly treated. Familiarity with the epidemiology, pathogenesis, clinical manifestations, imaging features, and treatment of hepatic infections can aid in radiologic diagnosis and guide appropriate patient care.

Abbreviations: ADC = apparent diffusion coefficient, HIV = human immunodeficiency virus, PCR = polymerase chain reaction

RadioGraphics 2016; 36:0000–0000

Published online 10.1148/rg.2016150196

Content Codes: CT GI US

[1]From the Department of Radiology, School of Medicine, Pontificia Universidad Católica de Chile, Marcoleta 367, 2nd Floor, Santiago 8330024, Chile (P.B., M.J.B., I.B., E.Z., M.V., A.H.); Department of Radiology, Mayo Clinic, Scottsdale, Ariz (C.M.); and Mallinckrodt Institute of Radiology, Washington University School of Medicine, St Louis, Mo (R.L., S.C., S.B.). Recipient of a Magna Cum Laude award for an education exhibit at the 2014 RSNA Annual Meeting. Received June 22, 2015; revision requested November 13 and received December 20; accepted February 20, 2016. For this journal-based SA-CME activity, the authors, editor, and reviewers have disclosed no relevant relationships. **Address correspondence to** A.H. (e-mail: *iahuete@med.puc.cl*).

SA-CME LEARNING OBJECTIVES

After completing this journal-based SA-CME activity, participants will be able to:

- Identify the most common imaging findings of infectious liver diseases, including bacterial, viral, parasitic, and fungal infections.
- Describe key imaging and clinical features that may help narrow the differential diagnosis of infectious liver diseases.
- Recognize potential pitfalls in image interpretation of liver infections.

See www.rsna.org/education/search/RG.

Introduction

Imaging plays an important role in the early detection, characterization, and management of infectious liver disease. Prompt diagnosis and management are crucial, especially for pyogenic and fungal infections because they can be fatal if not treated early. Ultrasonography (US), computed tomography (CT), and magnetic resonance (MR) imaging allow accurate detection of most hepatic infections, sometimes providing clues to identify the underlying pathogen.

However, the imaging features of hepatic infections may be less specific, and other conditions such as neoplasms, cysts, or autoimmune diseases may have similar features. Therefore, correct and timely diagnosis requires recognizing the unique imaging features that may be produced by certain pathogens and correlating them with the appropriate clinical and laboratory information. Nonetheless, it may be difficult to differentiate hepatic infections from other entities on the basis of imaging findings alone, and cultures from tissue sampling or fluid aspiration will occasionally be needed to ensure a confident final diagnosis and guide specific antimicrobial therapy.

TEACHING POINTS

- Although in some cases it may be extremely challenging to differentiate an abscess from a necrotic hepatic tumor, key imaging findings in abscesses are *(a)* the layered-wall appearance, with early inner rim enhancement that persists in delayed phases and progressive delayed enhancement of the outer layer; and *(b)* transient areas of segmental enhancement.
- Cholangitic microabscesses may mimic cysts because they can be markedly hyperintense on T2-weighted images. However, microabscesses usually show perilesional edema on T2-weighted images and a faint enhancing rim or restriction on diffusion-weighted images, features that are not present in typical liver cysts.
- Although the imaging findings in patients with viral hepatitis are not specific, imaging plays an important role to exclude other pathologic conditions with clinically similar manifestations, such as bile duct obstruction, diffuse metastatic disease, and cirrhosis.
- A multiloculated cystic biliary cystadenoma or cystadenocarcinoma shows enhancement of its internal septa and wall nodules, in contrast to the avascular nature of hydatid cysts.
- Intrahepatic cholangiocarcinoma, metastatic disease, and locally advanced gallbladder carcinoma may have a similar imaging appearance to that of hepatobiliary fascioliasis. However, linear tracts and, more importantly, eosinophilia should prompt consideration of possible fascioliasis.

In this article, we describe the most common imaging findings of bacterial, viral, parasitic, and fungal hepatic infections and review key imaging and clinical features that may help the radiologist narrow the differential diagnosis and avoid pitfalls in image interpretation.

Bacterial Infections

Bacterial infections of the liver can be categorized into three entities: *(a)* pyogenic liver abscesses, *(b)* bacterial granulomatous liver disease (eg, tuberculous liver disease and bartonellosis), and *(c)* acute bacterial hepatitis (1). The last condition is rare and usually shows either no imaging abnormalities or nonspecific findings.

Pyogenic Abscess

Liver abscess is the most common type of visceral abscess (2). Clinical manifestations include a broad spectrum of symptoms, but the most common are fever (70%–90% of patients) and abdominal pain, usually in the right upper quadrant (50%–75%) (3–5). The pathogenesis of liver abscesses is multifactorial; they can result from ascending cholangitis, hematogenous dissemination from a gastrointestinal infection via the portal vein or disseminated sepsis via the hepatic artery, or contiguous spread. Another route of bacterial liver seeding is direct inoculation, from either penetrating trauma or an invasive procedure (eg, biliary instrumentation, transcatheter arterial chemoembolization, percutaneous liver biopsy, percutaneous radiofrequency ablation, or abdominal surgery) (1).

Many bacteria have been described in the pathogenesis of pyogenic abscesses, reflecting the variability among patients and geographic areas. The majority of aspirated fluid cultures are positive, whereas blood cultures are positive in only 50% of cases (5). Most pyogenic liver abscesses are polymicrobial (5). Traditionally, *Escherichia coli* has been reported as the most common isolated microbe; however, recent data show that *Klebsiella pneumoniae* is the most common pathogen in pyogenic liver abscesses (4–6).

Management of pyogenic liver abscesses includes imaging-guided drainage and antibiotic therapy. There is considerable variation in clinical practice with regard to total antibiotic duration (7). It is recommended that antibiotic therapy be continued for at least 4–6 weeks, but the optimal duration is still unclear (7). Although drainage of single abscesses with a diameter of 5 cm or less can be achieved in some cases, it may not improve outcomes compared with antibiotic treatment alone. In isolated abscesses with a diameter greater than 5 cm, catheter drainage should be considered and is preferred over needle aspiration (8), although some favor surgical intervention. Prompt diagnosis and imaging-guided drainage have been reported to reduce mortality from 65% to 2%–12% (3–5).

The US and CT sensitivities for diagnosis of pyogenic liver abscess are 85% and 97%, respectively (9,10). At US, microabscesses (<2 cm) appear as hypoechoic nodules or ill-defined areas of distorted hepatic echogenicity (11). Large abscesses range from hypoechoic to hyperechoic masses, depending on the presence of internal echoes due to thickened septa and debris (11,12). Because echogenicity varies, a pyogenic abscess may simulate a solid lesion (Fig 1) (13). *K pneumoniae* monomicrobial liver abscesses are associated with a predominantly solid appearance at US (14). The ability to differentiate an abscess from a neoplasm at nonenhanced US is limited compared with CT or MR imaging. Acoustic through-transmission and absence of internal Doppler US signal in a hepatic abscess can aid in the exclusion of a solid neoplasm (Fig 1) (12,13). However, if a solid neoplasm has extensive necrosis, it may be indistinguishable from an abscess at US.

Several CT features and imaging signs of hepatic abscesses have been reported in the literature (9,15–18). The most common finding at contrast-enhanced CT is a well-defined, low-attenuation, round mass with an enhancing peripheral rim. Abscesses can manifest as a single nonloculated fluid collection, a single multilocu-

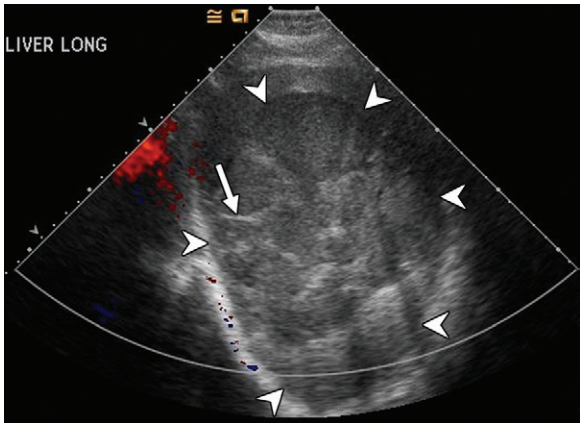

Figure 1. Bacterial hepatic abscess in a 52-year-old woman who presented with fever of unknown origin. Longitudinal color Doppler US image of the liver shows a hypoechoic mass (arrowheads) with internal echoes produced by echogenic septa (arrow) and debris. Note the absence of internal Doppler signal. Pathologic analysis of the liver biopsy specimen confirmed a multimicrobial abscess.

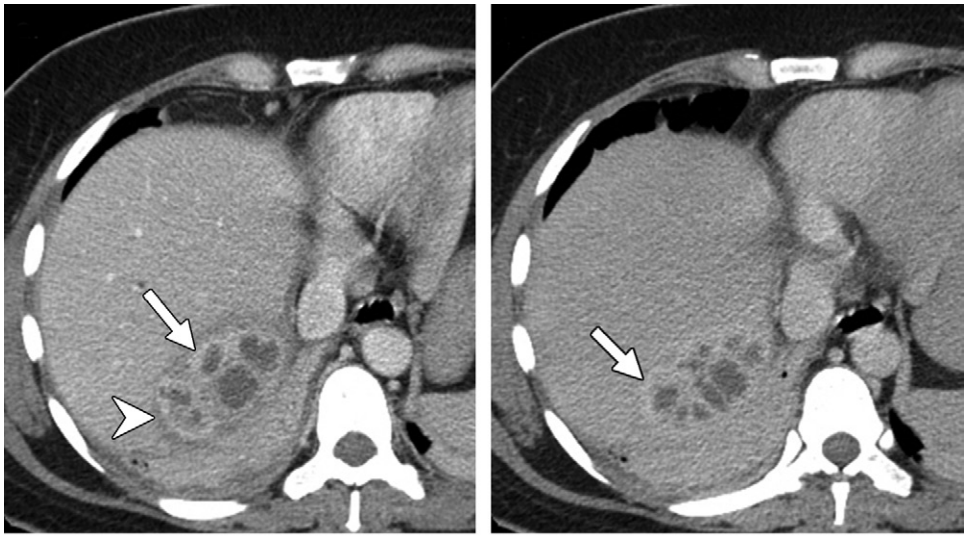

a. **b.**

Figure 2. Pyogenic liver abscess in a 45-year-old woman who presented with fever and pleuritic chest pain. **(a)** Axial contrast-enhanced portal phase CT image shows a multilocular cystic mass in the posterior segment of the right hepatic lobe abutting the right hemidiaphragm. Note the layered wall ("double target sign"), with an internal enhancing pyogenic membrane (arrow) surrounded by hypoattenuating parenchymal edema (arrowhead). **(b)** Axial contrast-enhanced delayed phase CT image shows persistent enhancement of the inner layer, delayed enhancement of the outer layer (arrow), and a confluence of multiple small locules producing the "cluster sign."

lated cystic mass, a solid (phlegmonous) process, or multifocal lesions (9,12,18). The "double target sign" is a characteristic imaging feature of hepatic abscess seen on contrast-enhanced CT images when a central low-attenuation fluid-filled area is surrounded by a high-attenuation inner ring and a low-attenuation outer ring (17). The inner layer shows early contrast enhancement that persists in delayed phases, as opposed to the outer layer, which is low attenuating in the early arterial phase and enhances only in delayed phases (Fig 2). The inner layer represents the pyogenic membrane, and the outer layer is due to edema of the hepatic parenchyma.

The "cluster sign" is also an imaging feature of pyogenic abscesses and occurs when multiple small low-attenuation lesions aggregate in a localized area and coalesce into a single larger abscess cavity (Fig 2) (16). A transient, early, wedge-shaped or circumferential segmental region of hepatic hyperenhancement at dynamic CT and MR imaging, which equilibrates in late phases, has also been reported to be associated with hepatic abscesses (15,19). This transient hepatic attenuation or signal intensity difference is thought to arise from inflammatory cell infiltration and stenosis or compression of small portal venules surrounding the hepatic abscesses, which may result in reduction of portal flow and a compensatory increase in arterial inflow (15). It is important to differentiate abscesses with transient segmental enhancement from tumors associated with segmental enhancement caused by portal or hepatic vein stenosis or occlusion (15). Careful

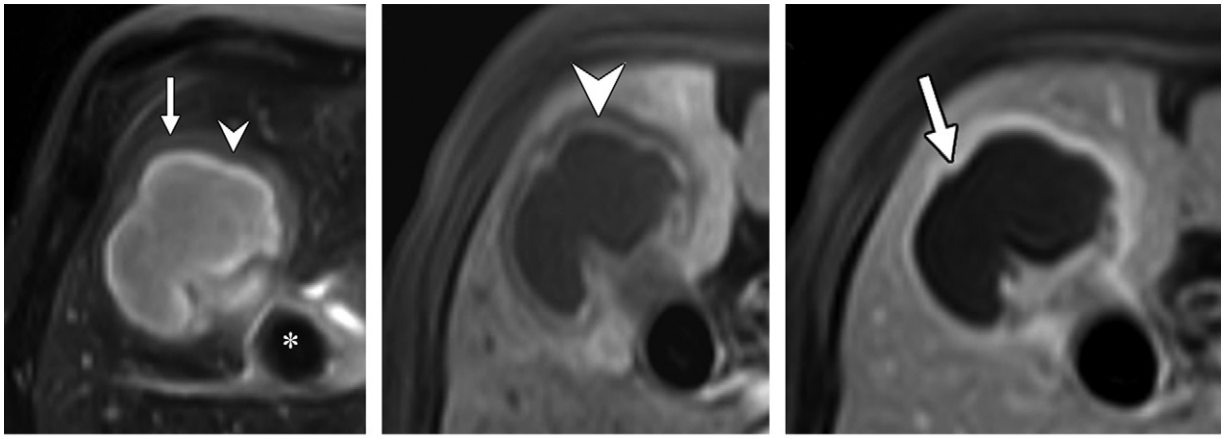

Figure 3. Pyogenic liver abscess from acute gangrenous cholecystitis in a 65-year-old man. **(a)** Axial T2-weighted MR image shows the double target sign of the abscess wall, seen as an iso- to hypointense inner layer (arrowhead) and a moderately hyperintense outer layer (arrow) surrounding the internal high-signal-intensity content of the abscess. Note the impacted hypointense stone in the gallbladder neck (*). **(b)** Axial contrast-enhanced arterial phase fat-suppressed T1-weighted MR image shows early enhancement of the inner layer (arrowhead) and adjacent segmental hepatic parenchymal hyperemia. **(c)** Axial contrast-enhanced delayed phase T1-weighted MR image shows delayed enhancement of the inner and outer layers (arrow).

CT and/or MR imaging evaluation of the index lesion is indispensable to differentiate these types of transient hepatic enhancement.

At MR imaging, abscesses typically show central low T1-weighted and high T2-weighted signal intensity (19,20), but internal signal intensity may vary depending on the protein content. The double target sign is denoted on T2-weighted images by an iso- to hypointense inner layer and a hyperintense outer layer (Fig 3a). Dynamic contrast enhancement is identical to that at CT, with early enhancement of the inner layer that persists in the delayed phase, and delayed enhancement of the periphery (Fig 3b, 3c) (19). Perilesional edema manifests as high signal intensity on T2-weighted images and can be identified in 35% of hepatic abscesses (20). High signal intensity on diffusion-weighted images and hypointensity on apparent diffusion coefficient (ADC) maps is generally seen (21).

Gas may be present in up to 20% of liver abscesses (9,22), either in the form of bubbles or as an air-fluid level, allowing a high degree of confidence in the diagnosis. Nevertheless, nonseptic gas formation may be seen in areas of liver necrosis, such as after liver tumor ablation, and can be a potential pitfall (23). At US, gas is seen as intense echogenic foci with posterior acoustic reverberations and shadowing (11). At MR imaging, gas can manifest as signal voids within an abscess (24), better depicted on T1-weighted gradient-echo images with a long echo time (in-phase images) because of the magnetic susceptibility of gas (Fig 4). Air-fluid levels are more common in *K pneumoniae* abscesses (25). An additional imaging feature of *K pneumoniae* infection is the "turquoise sign" due to numerous thin arborizing internal bands that resemble the turquoise mineral (Fig 5) (25).

Differential Diagnosis and Potential Pitfalls

Hepatic Tumor.—A solid organizing hepatic abscess may mimic a liver tumor (26). This is explained by absorption of necrotic pus and central collapse of the residual double-layered wall. However, abscesses still follow the contrast-enhancement kinetics (and signal intensity at MR imaging) of an inflammatory capsule with the double target sign (Fig 6), including progressive contrast material uptake in the outermost layer of the wall, a finding that favors an inflammatory origin over metastases or primary malignant hepatic tumors such as cholangiocarcinoma or hepatocellular carcinoma (26).

Intrahepatic cholangiocarcinoma or metastases may show a layered-wall appearance, which makes distinction from a solid organizing abscess difficult. Nevertheless, cholangiocarcinoma and desmoplastic adenocarcinoma metastases usually manifest with central progressive enhancement and simultaneous capsular washout, rendering their peripheral rim hypoattenuating or hypointense in comparison with the central core at portal and equilibrium phase imaging. Areas of segmental enhancement and perilesional edema surrounding organizing abscesses, or associated findings of intrahepatic cholangiocarcinoma (eg, capsular retraction, biliary duct dilatation upstream to the mass, or lobar or segmental atrophy), are helpful ancillary features that may help differentiate these entities. In some cases, differentiation

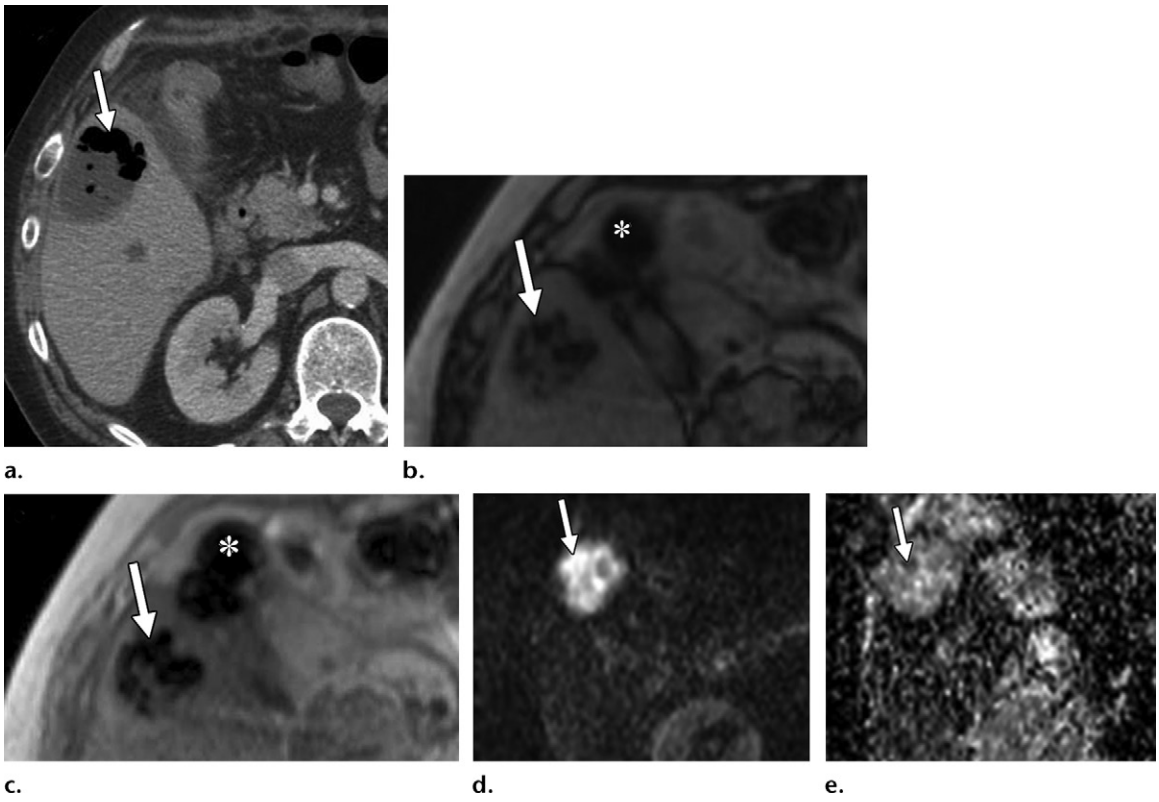

Figure 4. Extended-spectrum β-lactamase producing *K pneumoniae* abscess in a 55-year-old man 1 year after orthotopic liver transplant. **(a)** Axial contrast-enhanced CT image shows gas within a pyogenic liver abscess (arrow). **(b)** Axial gradient-echo opposed-phase T1-weighted MR image (echo time, 2.2 msec) shows signal void from gas within the abscess (arrow), similar to the appearance of colonic gas (*). **(c)** Axial gradient-echo in-phase T1-weighted MR image (echo time, 4.4 msec) shows blooming artifact within the abscess due to enhanced magnetic susceptibility effects from gas (arrow). Artifact is also noted in the adjacent colon (*). **(d)** Axial diffusion-weighted MR image (b = 800 sec/mm^2) shows internal high signal intensity in the abscess (arrow) due to restricted water diffusion. **(e)** Corresponding ADC map demonstrates decreased water diffusivity as internal low signal intensity in the abscess core (arrow).

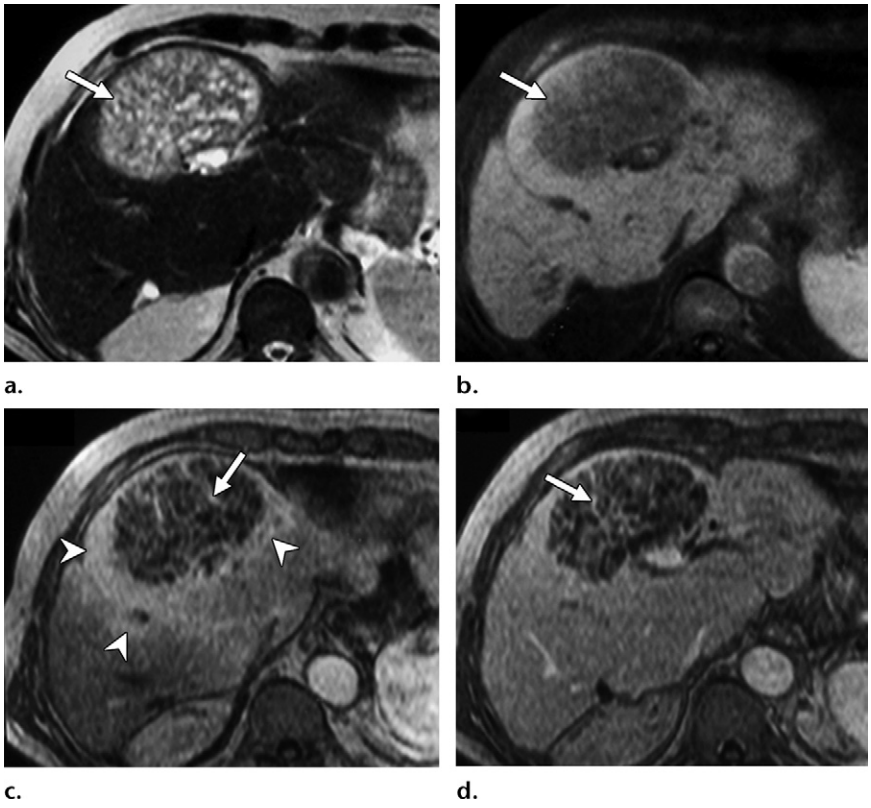

Figure 5. "Turquoise sign" and transient segmental enhancement in a hepatic abscess. **(a)** Axial T2-weighted MR image shows a focal liver abscess in the left hepatic lobe with internal high signal intensity and numerous arborizing septal bands (arrow) that resemble the turquoise mineral. **(b)** Axial nonenhanced fat-suppressed T1-weighted MR image shows a hypointense focal liver lesion (arrow). **(c)** Axial contrast-enhanced arterial phase T1-weighted MR image shows perilesional hyperenhancement (arrowheads) and enhancement of multiple internal septa (arrow). **(d)** Axial contrast-enhanced delayed phase T1-weighted MR image shows persistent enhancement of the internal septa (arrow). Cultures of the aspirated abscess contents grew *K pneumoniae.*

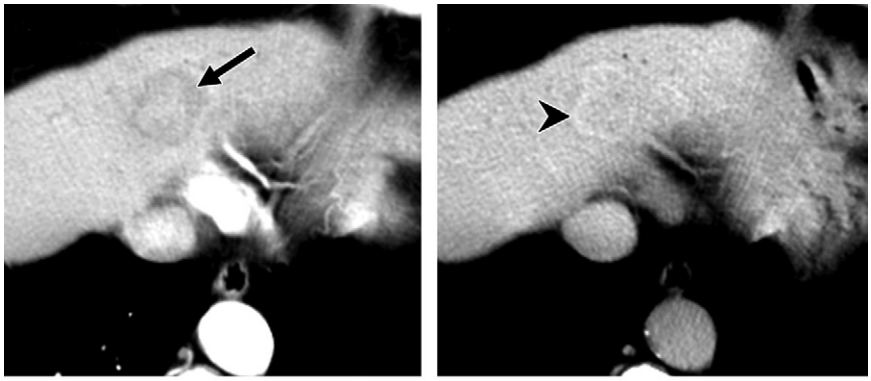

a. b.

Figure 6. Solid organizing liver abscess in a 69-year-old man with choledocholithiasis who presented with fever. **(a)** Axial contrast-enhanced CT image obtained in the early (arterial) phase shows a nodule with a "target" appearance, with a central early-enhancing area similar to the liver parenchyma and a low-attenuation rim (arrow). **(b)** Axial contrast-enhanced delayed phase CT image shows enhancement of the peripheral rim (arrowhead) surrounding an isoattenuating center. Note the absence of central fluid content due to pus absorption, which renders a solid appearance to the abscess. This lesion can be difficult to differentiate from an intrahepatic cholangiocarcinoma.

may not be possible and aspiration/biopsy must be performed.

Tumors with extensive necrosis may also mimic hepatic abscesses (21). However, the pattern of wall enhancement and signal intensity in tumors does not show the typical "target" appearance; the internal surface of the wall may also be more nodular in necrotic neoplasms (Fig 7). Moreover, a transient early circumferential or wedge-shaped segmental region of hepatic hyperenhancement and/or perilesional edema are often associated with abscesses.

In summary, although in some cases it may be extremely challenging to differentiate an abscess from a necrotic hepatic tumor, key imaging findings in abscesses are *(a)* the layered-wall appearance (17,26), with early inner rim enhancement that persists in delayed phases and progressive delayed enhancement of the outer layer; and *(b)* transient areas of segmental enhancement (15). Diffusion-weighted imaging and ADC maps may also help in differentiation (21). Abscesses generally show hyperintensity on diffusion-weighted images with high *b* values and hypointensity on ADC maps, in contrast to the cystic or necrotic portion of tumors, but there may be overlap (21,27).

Small Liver Cysts or Peribiliary Cysts.—Cholangitic microabscesses may mimic cysts because they can be markedly hyperintense on T2-weighted images. However, microabscesses usually show perilesional edema on T2-weighted images and a faint enhancing rim or restriction on diffusion-weighted images, features that are not present in typical liver cysts (Fig 8) (21).

Figure 7. Necrotic tumor mimicking a hepatic abscess in a 38-year-old woman who presented with right upper quadrant pain and low-grade fever. Coronal reformatted contrast-enhanced CT image shows a hypoattenuating mass with irregular internal septa in the right hepatic lobe. Although an abscess could be considered, wall features of internal nodularity and absence of a target appearance suggest a necrotic solid tumor. An internal focal calcification (arrow) also favors a neoplasm over an abscess. Pathologic analysis of a tissue sample showed the finding to be a necrotic poorly differentiated embryonal sarcoma.

Furthermore, peribiliary cysts usually are seen in patients with cirrhosis and follow the central portal tracts (28). It should be noted that biliary hamartomas may also show thin rim enhancement that is most conspicuous on delayed gadolinium-enhanced images (29). However, in cases of biliary hamartomas, neither perilesional edema nor restriction should be seen on diffusion-weighted images. From a clinical standpoint, patients with microabscesses usually have classic symptoms of cholangitis, including fever,

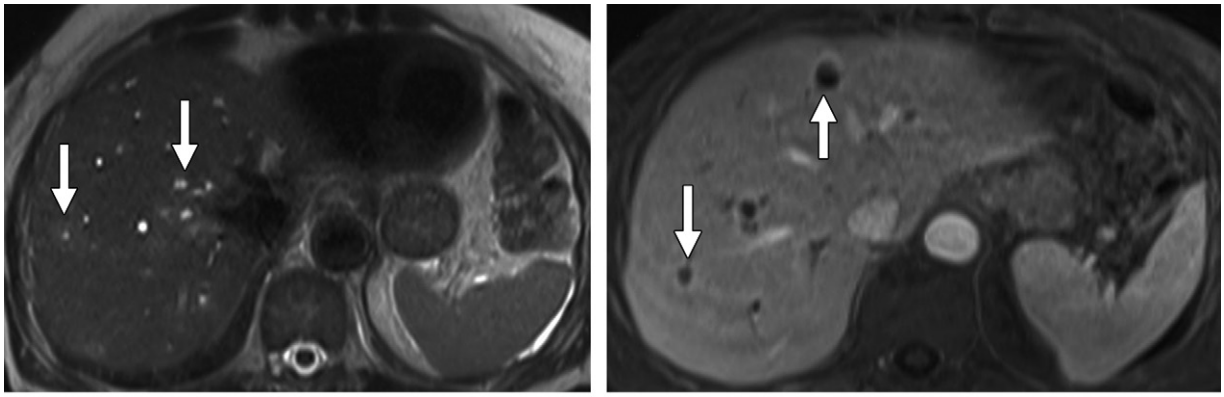

a. b.

Figure 8. Small cholangitic abscesses mimicking cysts in a 68-year-old woman with biliary obstruction from pancreatic adenocarcinoma who presented with jaundice and fever. **(a)** Axial T2-weighted MR image shows intermediate-signal-intensity perilesional edema surrounding hyperintense lesions (arrows). **(b)** Axial contrast-enhanced T1-weighted MR image shows faint rim enhancement of the lesions (arrows), a finding consistent with cholangitic microabscesses. Faint rim enhancement can be seen in cystic biliary hamartomas as well, but they are not associated with perilesional edema.

jaundice, and right upper quadrant pain, while patients with biliary hamartomas are asymptomatic. Restriction at diffusion-weighted imaging is the most useful feature to differentiate infected from noninfected cystic lesions (21).

Absorbable Hemostatic Material.—Absorbable sponges placed after surgical interventions such as hepatic resections or liver transplant to control excessive intraoperative bleeding may look similar to abscesses, appearing as focal pockets of air within a complex fluid collection (30). These can be detected in the surgical bed up to 1 month postoperatively (31). Correlation with clinical data and the surgical procedure should be enough to avoid misinterpretation. However, when clinical correlation is not feasible, distinction between the two entities can be difficult. Imaging features that favor an absorbable hemostatic sponge over an abscess are linear gas collections and low signal intensity on T2-weighted MR images (31).

Tuberculous Granulomatous Liver Disease

Tuberculosis corresponds to infection by *Mycobacterium tuberculosis.* Regardless of the number of advances in prevention, diagnosis, and treatment, tuberculosis remains one of the world's deadliest communicable diseases (32). Extrapulmonary tuberculosis with liver involvement is usually seen in immunocompromised patients with disseminated infection (33). Although various immunodeficiency disorders are predisposing risk factors for developing extrapulmonary tuberculosis, the incidence is higher in individuals infected by human immunodeficiency virus (HIV) with CD4 counts below 200 cells/μL (32).

Hepatic tuberculosis can manifest as a micronodular or macronodular form (34). Micronodular liver involvement, also known as miliary tuberculosis, is the most common form and results from hematogenous spread of *M tuberculosis* from a pulmonary or extrapulmonary source (34). This form is frequently associated with splenic involvement and miliary pulmonary tuberculosis (34). Micronodular tuberculosis is often not detected at imaging, and hepatomegaly may be the only abnormality (11). When focal liver lesions are detectable, sonography may reveal diffuse, tiny, nonspecific hypoechoic nodules (12). However, because the lesions are often too small to be seen, US may show only a diffusely hyperechoic liver (12). Micronodular tuberculosis may manifest as multiple tiny (0.5–2.0-mm) low-attenuation nodules with no discernible ring enhancement at CT (Fig 9) (24,34). With healing, small scattered calcifications can result. At MR imaging, micronodular lesions are hypointense on T1-weighted images and hyperintense on T2-weighted images (35). The differential diagnosis of micronodular tuberculosis includes disseminated fungal infections, bartonellosis, sarcoidosis, lymphoma, and metastases. Differentiation of these entities is difficult and sometimes not possible on the basis of imaging findings alone. Nevertheless, because liver tuberculosis is usually seen in disseminated infection, coexisting spleen involvement and necrotic abdominal lymph nodes should raise suspicion for mycobacterial infection. Moreover, when there is coexisting lung disease such as miliary infiltrates or cavitary pulmonary lesions, tuberculosis should be considered.

Macronodular hepatic tuberculosis is rare (24). Nodules may be single or multiple but are

fewer in number compared with the micronodular form. Typically, nodules are hypoechoic at US and hypoattenuating at CT, and a peripheral enhancing rim may be seen after contrast agent administration (24,36). At MR imaging, the nodules have low signal intensity on T1-weighted images, but on T2-weighted images they may show variable signal intensity (hypo- or hyperintense) depending on the stage of disease evolution (35,36). Because the imaging findings are not specific, diagnosis often requires culturing or detecting caseating granulomas of *M tuberculosis* in tissue samples or confirming tuberculosis with a polymerase chain reaction (PCR) test or acid-fast bacillus testing.

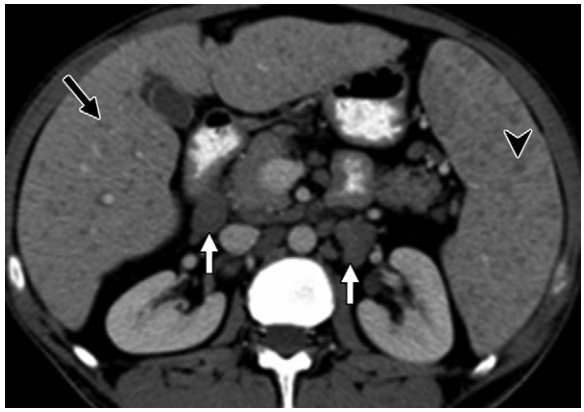

Figure 9. Disseminated tuberculosis infection in a 24-year-old man with HIV infection who presented with night sweats and fever. Axial contrast-enhanced CT image shows multiple tiny hypoattenuating lesions in the liver (black arrow) and spleen (arrowhead), findings associated with retroperitoneal adenopathy (white arrows).

Bartonellosis

Bartonellosis (cat-scratch disease) is an infection caused by *Bartonella henselae*, a gram-negative bacterium that is introduced into human hosts through a scratch or bite from a cat and most commonly affects children and young adults (37). Small red-brown papules may develop at the site of inoculation. Symptoms begin 1–3 weeks after the cat scratch or bite, with painful lymphadenopathy proximal to the site of inoculation and fever (38). Visceral involvement can occur in the absence of lymphadenopathy, manifesting as a fever of unknown origin (38). The diagnosis of bartonellosis is confirmed by serologic tests, PCR test, or biopsy (37,38).

Disseminated infection is seen in 5%–10% of cases (11,39). Hepatic bartonellosis is characterized by multiple necrotizing granulomas ranging from 3 to 30 mm, with or without hepatomegaly (11,38). At US, lesions can vary in appearance, but most commonly they are nonspecific hypoechoic nodules. At nonenhanced CT, the lesions are hypoattenuating relative to normal liver parenchyma (11,40). Three different patterns have been described at contrast-enhanced CT (40): *(a)* persistent hypoattenuation relative to the liver (Fig 10), *(b)* isoattenuation relative to surrounding tissues, and *(c)* faint rim enhancement. At MR imaging, hepatic bartonellosis nodules are hypointense on T1-weighted images and hyperintense on T2-weighted images, with faint rim enhancement (41), and there may be associated splenic nodules. These lesions share similar imaging features with other conditions, such as disseminated fungal infections, lymphoma, sarcoidosis, and metastases. Radiologists should consider hepatic bartonellosis in immunocompetent children and young adults without known malignancy who display multiple liver lesions and, occasionally, associated splenic nodules at imaging. However, confirmation often requires serologic analysis or tissue sampling. Although the disease may be self-limited, antimicrobial therapy is usually administered to speed recovery (38).

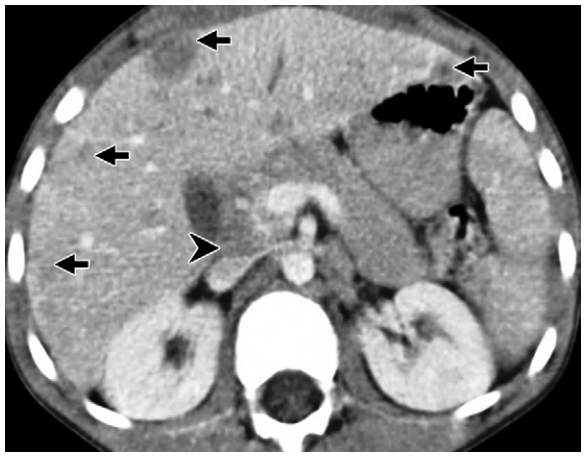

Figure 10. Hepatic bartonellosis in a 6-year-old boy who presented with 3 weeks of fever after a witnessed cat scratch. Axial contrast-enhanced CT image shows multiple hypoattenuating liver nodules (arrows) and associated periportal lymph nodes (arrowhead). The lesions may be indistinguishable from metastases. However, multiple liver lesions seen in an immunocompetent young patient without a known malignancy should raise the possibility of hepatic bartonellosis.

Infection by *B henselae* in patients with HIV infection may cause bacillary peliosis (42) (from the Greek *pelios*, meaning dusky or purple). Peliosis is a rare benign vascular condition that may simulate hemangiomas or other vascular tumors (42). At US, multiple small, round, hypoechoic lesions can be seen in the liver and spleen. CT may demonstrate multiple low- or high-attenuation lesions scattered throughout the hepatic parenchyma, and T2-weighted MR imaging shows hyperintense focal lesions (42). Enhancement may be globular, centripetal, or centrifugal, but it usually is continuous, with no

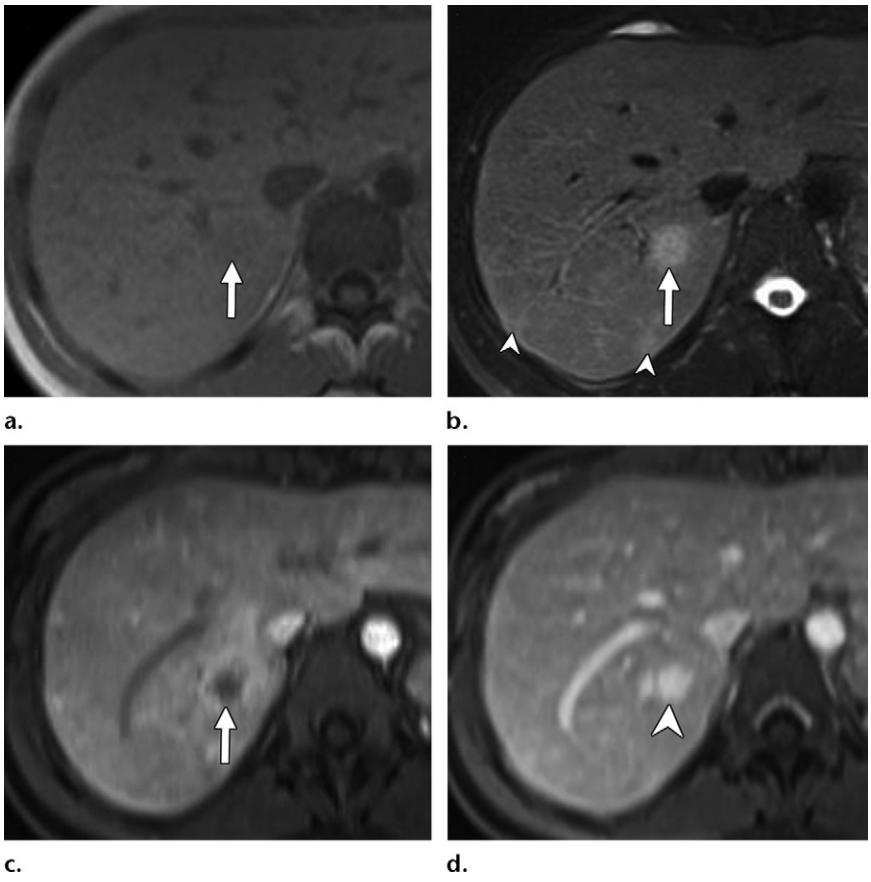

Figure 11. Bacillary peliosis in a 32-year-old man with HIV/AIDS who presented with fever. **(a)** Axial in-phase T1-weighted MR image shows an ill-defined iso- to mildly hypointense nodule in the posterior segment of the right hepatic lobe (arrow). **(b)** Axial fat-saturated T2-weighted MR image shows moderate to high signal intensity of the nodule (arrow). Smaller similar subcapsular nodules are seen posteriorly (arrowheads). **(c)** Axial contrast-enhanced early phase fat-suppressed T1-weighted MR image shows the hypointense right hepatic nodule with irregular continuous peripheral enhancement (arrow). **(d)** Axial contrast-enhanced delayed phase T1-weighted MR image shows delayed enhancement within the nodule (arrowhead), which reaches a signal intensity similar to that of the surrounding hepatic venous structures because of contrast agent retention within dilated sinusoids in the lesion.

washout in delayed phases because of accumulation of contrast agent in dilated hepatic sinusoids. Therefore, lesions remain slightly hyperattenuating at CT and slightly hyperintense at MR imaging compared with the surrounding liver on portal venous phase images (Fig 11) (42,43). There is little or no mass effect on neighboring hepatic vessels. The differential diagnosis includes hemangiomas, hypervascular metastases, and well-differentiated primary hepatic angiosarcoma. Hemangiomas show globular discontinuous contrast enhancement, as opposed to peliosis, where initial peripheral enhancement is usually continuous. However, in some cases, differentiation can be difficult on the basis of imaging findings alone. Hypervascular metastases and well-differentiated primary hepatic angiosarcoma are typically hypo- to isoattenuating to liver parenchyma on portal venous phase images (43). Clinical history is also helpful to suggest the diagnosis of bacillary peliosis. Although hepatic peliosis can be seen in a variety of settings, hepatic peliosis secondary to *B henselae* infection is usually described in patients with HIV/AIDS.

Viral Infections

Acute viral hepatitis is usually caused by hepatitis A, B, C, or E viruses (44). Other viruses known to cause hepatitis include hepatitis D virus (which requires coexisting hepatitis B virus infection), HIV, coxsackievirus, and herpes simplex viruses. Although herpes hepatitis is rare, it can be seen in immunosuppressed and pregnant patients.

Clinical manifestations vary, as patients may be asymptomatic or may present with fever, abdominal discomfort, and jaundice (44). Other less common manifestations include acute fulminant liver failure, subclinical infection leading to chronic cirrhosis, and rapidly progressive infection resulting in cirrhosis.

The diagnosis of viral hepatitis is usually made on the basis of clinical presentation, serology, PCR test, or immunohistochemistries at histopathologic analysis. Although the imaging findings in patients with viral hepatitis are not specific, imaging plays an important role to exclude other pathologic conditions with clinically similar manifestations, such as bile duct obstruction, diffuse metastatic disease, and cirrhosis (11).

Imaging features of acute viral hepatitis at US include hepatomegaly with decreased parenchymal echogenicity, which results in a relative increase in the echogenicity of the portal triads (45) and gives a "starry sky" appearance (11). At CT, periportal edema, heterogeneous enhance-

ment, and well-defined regions of low attenuation may be present. At MR imaging, these regions are hypointense on T1-weighted images and hyperintense on T2-weighted images (11). It should be noted that acute viral hepatitis can manifest with normal liver findings at imaging (45).

Extrahepatic findings in patients with acute viral hepatitis include gallbladder wall thickening due to edema (up to 70% of patients), which may be striking and may simulate acute cholecystitis (46). However, in patients with acute cholecystitis, the gallbladder lumen is distended, in contrast to patients with acute hepatitis, where luminal collapse may be seen (Fig 12).

Fulminant hepatic failure, defined as the development of encephalopathy within 8 weeks of symptom onset in a patient with a previously healthy liver (44), can result in confluent fibrosis or scarring at follow-up CT and MR imaging. Calcifications may also develop in the affected regions (47).

Although the liver may also appear normal in chronic viral hepatitis, a coarsened hepatic echotexture and increased parenchymal echogenicity can be seen at US (11,24). CT and MR imaging features may resemble those of early-stage liver cirrhosis (11).

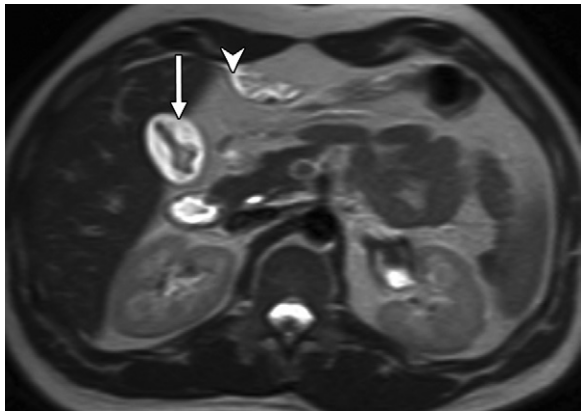

Figure 12. Acute viral hepatitis in a 28-year-old man who presented with cholestatic jaundice. Axial T2-weighted MR image shows marked gallbladder wall thickening (arrow) due to edema, with secondary luminal collapse. Periportal edema with extension to the falciform ligament is also seen (arrowhead).

Parasitic Infections

Amebic Abscess

Amebic liver abscess is the most common extraintestinal complication of *Entamoeba histolytica* infection. This protozoan infection is endemic in Africa, Southeast Asia, and Central and South America (24,48).

Patients with amebic liver abscess are usually adult and male (10 times more common in men than women). Clinical manifestations of liver infection are right upper quadrant pain, fever, cough, and hepatomegaly. Diagnosis requires detection of *E histolytica*–specific antigen or DNA in stool specimens and antiamebic antibodies in blood serum (48).

Metronidazole therapy is the mainstay of medical treatment and is sufficient to eradicate the disease in most patients, even with just one dose (48). Aspiration is generally unnecessary in patients with amebic liver abscess (48) but should be considered in individuals in whom the diagnosis is uncertain (where pyogenic abscess or bacterial superinfection of the amebic liver abscess is a concern), in patients who have a failed response to metronidazole therapy (persistent fever or pain after 4 days of treatment), and in patients with large abscesses at high risk for rupture (especially rupture into the pleura or pericardium) (48). Resolution of abscesses at imaging may take up to 2 years after resolution of clinical manifestations; therefore, persistent imaging abnormalities should not prompt reinstitution of therapy or further testing in clinically well patients (49).

At imaging, amebic liver abscess is classically unilocular, although septa may be present in 30% of cases (50). About 70%–80% of lesions are solitary and are located in the right hepatic lobe, typically near the liver capsule, and may be indistinguishable from a unilocular pyogenic abscess (50). At US, it appears as a hypoechoic and homogeneous round or oval mass, with low-level internal echoes, no noticeable wall echoes, and distal through-transmission (12,51). A focal liver lesion in combination with diaphragmatic disruption is highly suggestive of amebic liver abscess (50,51).

At contrast-enhanced CT, an amebic liver abscess is a well-defined lesion with complex fluid-attenuation values and rim enhancement (50). Its capsule may also demonstrate a "target" or "double-rim" appearance (Fig 13). Extrahepatic extension is common (50,51). MR imaging findings simulate those of other pyogenic abscesses, with low signal intensity on T1-weighted images and high signal intensity on T2-weighted images, and are frequently associated with perilesional edema (52).

Echinococcus Infection

Echinococcosis is a worldwide zoonosis produced by ingestion of food or water contaminated with eggs of the *Echinococcus* tapeworm. The most common forms of human echinococcosis are cystic and alveolar echinococcosis (53).

Cystic echinococcosis (hydatid disease) is the most common form and is caused by *Echinococcus granulosus*, a tapeworm with worldwide distribution. The liver is the most common organ involved

Figure 13. Amebic liver abscess in a 44-year-old woman who presented with fever and right upper quadrant pain 3 weeks after a trip to Central America. Axial contrast-enhanced CT image shows a well-defined hypoattenuating lesion in the right hepatic lobe, with a "target" or "double-rim" appearance of its thick peripheral wall (arrow). Serologic tests were positive for *E histolytica.* An amebic abscess can mimic a unilocular pyogenic abscess.

(70%–75%) (53). Patients may be asymptomatic, especially when the cyst is small. Larger cysts may produce abdominal pain, a palpable right upper quadrant mass, or obstructive jaundice (12,53). Anaphylaxis and seeding to other parts of the body may manifest with cyst rupture. Bacterial superinfection of cysts and development of a hepatic abscess have been also described (53).

The mature hydatid cyst consists of three layers (11,54): *(a)* the endocyst (inner or germinal layer), the living tissue that surrounds the fluid-filled central hydatid cavity; *(b)* the ectocyst (middle layer), an acellular laminated membrane secreted by the germinal membrane; and *(c)* the pericyst (outer layer), a thick fibrous capsule corresponding to the host response of the liver parenchyma. Daughter cysts may be present within the cyst and are the result of endocyst invagination (11). They are a marker of cyst viability. If a daughter cyst ruptures, scolices pass into the cyst fluid and form white sediment known as hydatid sand (24).

Imaging features of cystic echinococcosis may be enough to establish the diagnosis, especially when daughter cysts are present. Detection of serum antibodies may aid in diagnosis, as sensitivity may be as high as 85%–98% for liver cysts, but the specificity of all tests is limited by cross reactions (53).

The US appearance of hydatid disease ranges from purely cystic to solid-appearing pseudotumors. The World Health Organization classification of hepatic hydatid cysts according to US findings is useful to assess the stage and guide appropriate management (53). Six stages have been described:

1. Cystic lesion (CL): An active unilocular cyst is seen with uniform anechoic content and a cystic wall that is not clearly visible.

2. *E granulosus* cyst (CE) type 1: An active unilocular simple cyst is seen with uniform anechoic content and a well-visible cystic wall. When repositioning the patient, fine echoes due to hydatid sand can be seen to fall dependently ("snowstorm sign").

3. CE type 2: An active multivesicular multiseptated cyst with a well-defined wall is seen. Daughter cysts separated by the hydatid matrix may partly or completely fill the unilocular mother cyst in a "spoke-wheel" pattern.

4. CE type 3: An active unilocular cyst is seen with an inner, floating, detached membrane ("water lily sign"). The water lily sign is explained by a decrease in intracystic pressure due to loss of the parasite's viability.

5. CE type 4: A cyst with mixed hypo- and hyperechoic contents (pseudotumor appearance) is seen with absent daughter cysts. It may manifest as the "ball of wool sign" indicative of degenerating membranes (Fig 14). Most cysts of this type are inactive (nonviable).

6. CE type 5: Cysts at this stage are characterized by a partially or complete calcified wall. Partial calcification does not always indicate cyst death, but complete calcification of the wall and central contents usually indicates a nonviable cyst (24,53).

Similar to the US findings, the CT findings correspond to the stage of cyst growth: unilocular, with daughter cysts, partially calcified, or densely calcified. The cyst wall can show high attenuation on nonenhanced images, and daughter cysts show lower attenuation than the main cyst (Fig 15). Detached endocyst membranes (water lily sign) can show linear areas of high attenuation (54). A densely calcified cyst is, again, a marker of nonviability.

MR imaging best demonstrates the pericyst, matrix or hydatid sand (debris consisting of freed scolices), and daughter cysts (11) (Fig 16). On T1- and T2-weighted images, the pericyst appears as a hypointense rim because of its fibrous composition and calcifications. The hydatid matrix shows intermediate to low signal intensity on T1-weighted images and intermediate to high signal intensity on T2-weighted images (55). When present, daughter cysts show higher signal intensity on T2-weighted images relative to the matrix (54), with a signal intensity approaching that of bile or cerebrospinal fluid (Fig 16). After contrast agent administration, there is no enhancement of the cyst contents, including the visible septa. The fibrous pericyst may demonstrate mild delayed contrast enhancement. Some hydatid cysts may

contain air-fluid levels or fat globules (Fig 17) (54). Intracystic fat is thought to derive from the lipid elements in bile, implying that there is a communicating rupture. Care must be taken not to confuse it with fat-containing hepatic neoplasms such as a hepatocellular adenoma or carcinoma (both are solid and usually hypervascular).

Treatment of cystic echinococcosis includes antiparasitic agents such as albendazole or mebendazole, surgery (pericystectomy), and/or percutaneous drainage with injection of a protoscolicidal substance (preferably 95% ethanol).

Differential Diagnosis and Potential Pitfalls

Biliary Cystadenoma or Cystadenocarcinoma.—A multiloculated cystic biliary cystadenoma or cystadenocarcinoma shows enhancement of its internal septa and wall nodules, in contrast to the avascular nature of hydatid cysts (Fig 18) (56). However, when septal calcifications are present in biliary cystadenoma or cystadenocarcinoma, it may not be possible to identify definite septal enhancement.

Complicated or Hemorrhagic Liver Cyst or Giant Bile Duct Hamartoma.—High signal intensity on T1-weighted images helps distinguish a complicated or hemorrhagic liver cyst or a giant bile duct hamartoma from hydatid disease (Fig 19). A giant bile duct hamartoma has a propensity to bleed (57), but bleeding into a hydatid cyst is an extremely rare complication (58).

Simple Liver Cyst.—A unilocular hydatid cyst is rare but may appear identical to a liver cyst (59). The following imaging findings may be the only clues for diagnosis: hydatid sand, focal or segmental thickening of the cyst wall, coexistent echinococcal cysts in the spleen or lungs, pericystic biliary dilatation, segmental or lobar liver atrophy, satellite cysts, and elongated cyst shape (59). However, differentiation of these two entities is challenging and sometimes is not feasible.

Fascioliasis

Hepatobiliary fascioliasis is caused by the trematode *Fasciola hepatica*. The main source of infestation is ingestion of watercress or similar green vegetables on which the infective metacercaria forms of the parasite are attached. Fascioliasis is endemic in some regions of South America, Cuba, Egypt, Iran, and Turkey and in parts of western Europe (60).

Infection in the definitive host is divided into two phases: the parenchymal/hepatic (migratory) phase and the biliary phase. In the parenchymal phase, hatched juvenile flukes penetrate the intestinal wall and then migrate within the peritoneal cavity and penetrate the liver capsule (61,62).

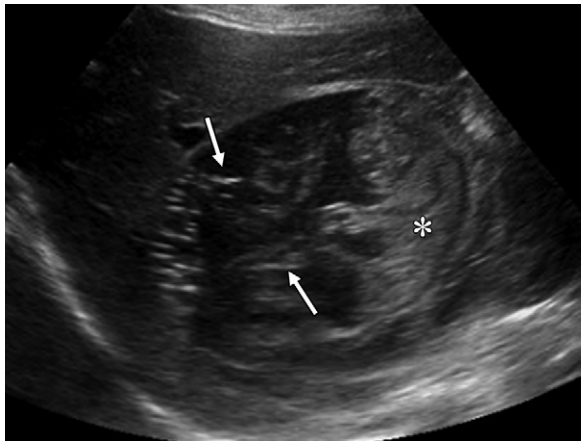

Figure 14. Liver hydatid cyst in a 31-year-old woman who presented with right upper quadrant pain. Transverse US image of the right hepatic lobe shows a heterogeneous mass (*) with mixed hypo- and hyperechoic contents ("pseudotumor" appearance) and degenerating membranes (arrows) floating within the cyst cavity ("ball of wool sign").

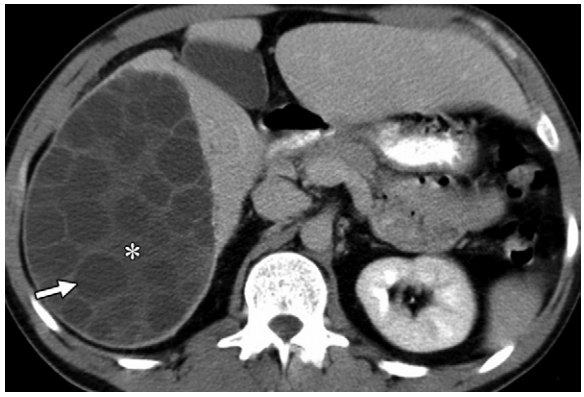

Figure 15. Hepatic hydatid cyst in a 42-year-old man from South America who presented with right upper quadrant pain. Axial contrast-enhanced CT image shows classic features of a hydatid cyst, with multiple hypoattenuating daughter cysts within a large right hepatic cystic mass. Note that the daughter cysts (arrow) show lower attenuation than the cyst matrix (*).

During the liver fluke's migration, hepatic tissues are mechanically destroyed, and inflammation appears around their migratory tracts. The biliary phase begins when parasites enter the biliary ducts of the liver. In the biliary tree, the flukes mature and produce eggs.

Clinically, patients with fascioliasis present with right upper quadrant pain due to hepatic capsular irritation and subcapsular abscesses created by the parasites (62). Fever, weight loss, pruritus, and skin rashes may also occur. Blood eosinophilia occurs in the hepatic phase (62). Definitive diagnosis is made on the basis of serologic tests or visualization of eggs in endoscopically or percutaneously aspirated bile, liver tissue, or stool (60,62). Triclabendazole is the drug of choice recommended by the World Health Organization for treatment of fascioliasis (63). However, this

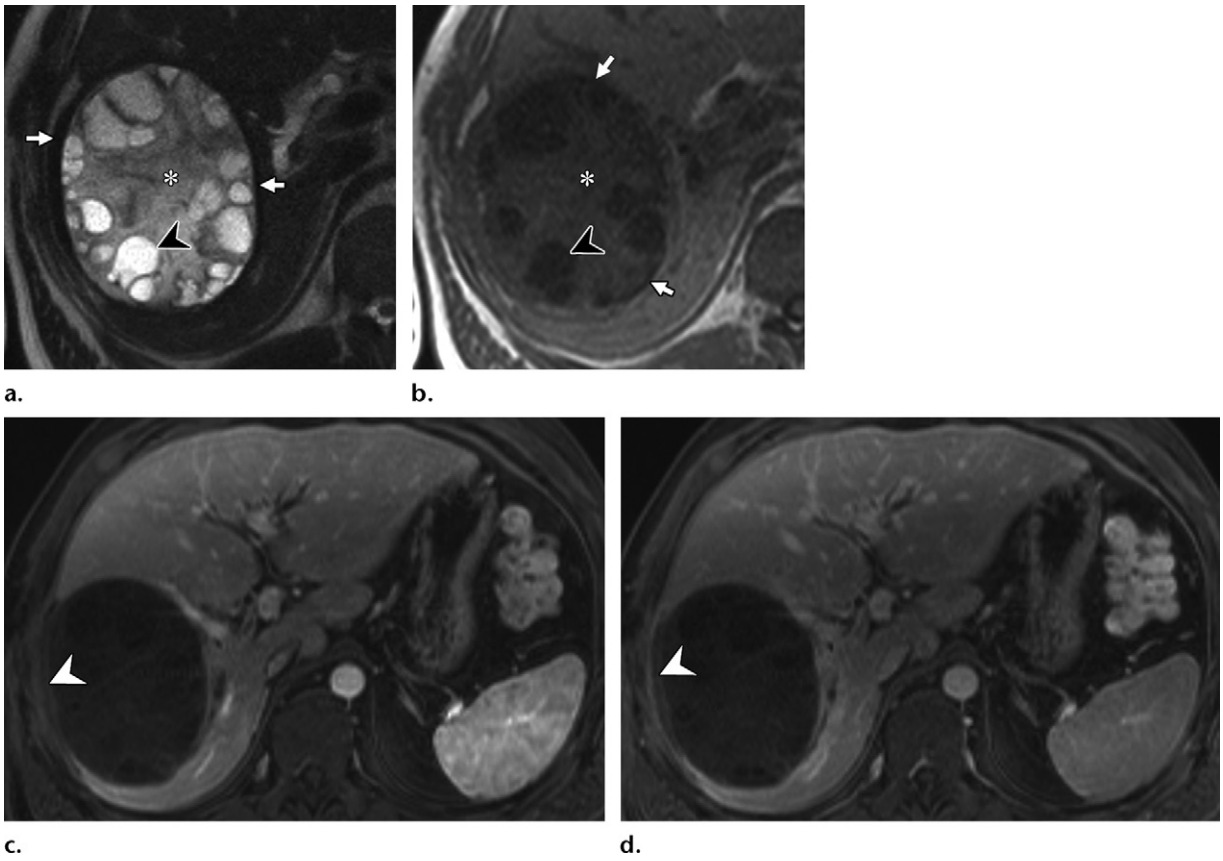

Figure 16. Hepatic hydatid disease in a 37-year-old man from Chile who presented with right subcostal pain. **(a)** Axial T2-weighted MR image shows a pericyst with a markedly hypointense rim (arrows) due to its fibrous composition. Capsular calcifications can also explain a low-signal-intensity pericyst. The hydatid matrix (*) shows intermediate signal intensity. Daughter cysts (arrowhead), when present, indicate a viable cyst and are T2-hyperintense relative to the underlying matrix. **(b)** Axial in-phase T1-weighted MR image shows the low-signal-intensity fibrous pericyst (arrows). The hydatid matrix (*) has intermediate signal intensity. Daughter cysts (arrowhead) are usually of lower T1 signal intensity relative to the hydatid matrix. **(c, d)** Axial contrast-enhanced fat-suppressed portal **(c)** and delayed **(d)** phase T1-weighted MR images show no enhancement of the cyst contents. The pericyst (arrowhead) shows mild contrast enhancement.

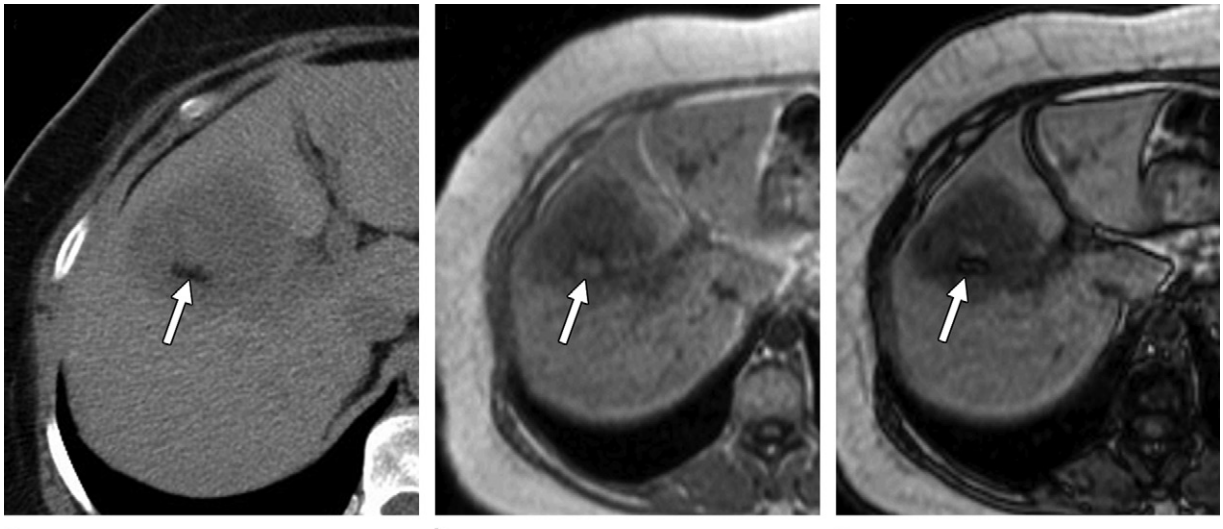

Figure 17. Fat-containing hydatid cyst in a 57-year-old woman who presented for evaluation of a liver lesion. **(a)** Axial nonenhanced CT image shows a macroscopic fat globule (arrow) within a liver lesion. Intracystic fat may derive from the lipid elements in bile and implies a communicating rupture. **(b)** Axial gradient-echo in-phase T1-weighted MR image shows a high-signal-intensity focus (arrow) within the lesion. **(c)** Axial gradient-echo opposed-phase T1-weighted MR image shows macroscopic fat within the cyst, a finding confirmed by chemical shift artifact and signal cancellation surrounding the lipid component (arrow).

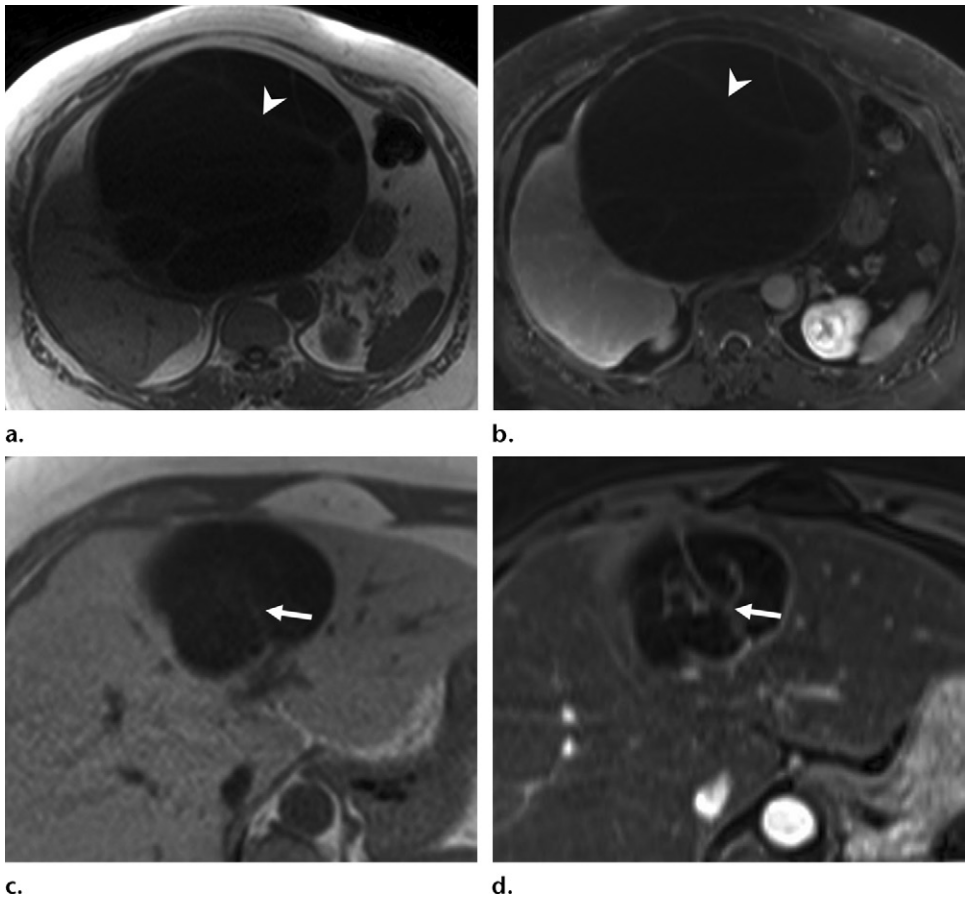

Figure 18. Hydatid cyst versus cystic hepatic tumor. **(a, b)** Hydatid cyst in a 49-year-old woman who presented with an abdominal mass. **(a)** Axial gradient-echo in-phase T1-weighted MR image shows a low-signal-intensity cystic liver lesion with septa (arrowhead). **(b)** Axial contrast-enhanced delayed T1-weighted MR image shows absence of intracystic enhancement and hypointense septa (arrowhead). **(c, d)** Biliary cystadenoma in a 57-year-old woman who presented for follow-up of an indeterminate liver lesion. **(c)** Axial gradient-echo in-phase T1-weighted MR image shows a lobulated cystic liver lesion with internal septa (arrow). **(d)** Axial contrast-enhanced fat-suppressed T1-weighted MR image shows irregular moderately enhancing internal septa (arrow), a helpful differentiating feature from hydatid cyst.

drug is not approved by the U.S. Food and Drug Administration. Nitazoxanide may be an alternative to triclabendazole, but more studies are needed on its efficacy and tolerability (60).

At US, patients with fascioliasis have subcapsular, confluent, ill-defined, hypoechoic nodules during the parenchymal phase (Fig 20). In the biliary phase, thickening of the gallbladder wall or common bile duct and mild intrahepatic biliary ductal dilatation due to cholangitis are frequently seen. The parasite(s) may be seen in the common bile duct or gallbladder as leaflike or curvilinear snail-like echoes measuring 5–25 mm that may move during US if alive (62).

At CT, multiple small (up to 2–3 cm in diameter), confluent, subcapsular nodules with ill-defined borders may be seen (Fig 21). These tend to converge toward the hepatic hilum following the central portal triads. Inflammatory low-attenuation tracts follow a linear path and are best depicted just deep to the liver capsule. Reactive lymph nodes and perihepatic fluid can be seen (62). Subcapsular hepatic hematoma is an infrequent but potentially lethal complication (64). At MR imaging, five patterns of fascioliasis have been described: *(a)* perihepatitis or capsular inflammation; *(b)* subcapsular-periportal ill-defined linear tracts (Fig 22); *(c)* segmental areas of hepatic inflammation with geographic borders; *(d)* abscess with rim enhancement; and *(e)* focal postinflammatory fibrosis (65). Tracts, parenchymal inflammation, and abscesses are characterized by hypointensity on T1-weighted images and hyperintensity on T2-weighted images and may show restricted diffusion on diffusion-weighted images (Fig 22d). Late fibrosis shows low signal intensity on T1- and T2-weighted images. MR cholangiography may show biliary parasites within the distal bile duct or gallbladder as ill-defined, elongated, hypointense filling defects (Fig 22e).

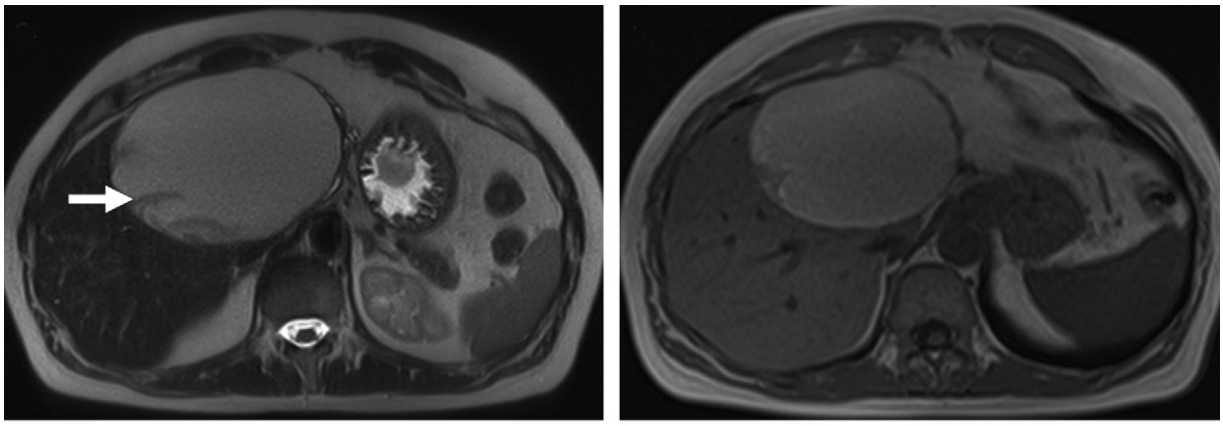

a. b.

Figure 19. Hemorrhagic liver cyst mimicking hydatid liver disease in a 51-year-old woman who presented with acute epigastric pain. **(a)** Axial T2-weighted MR image shows a large hepatic cyst with intermediate signal intensity and hypointense wavy bands (arrow) that may simulate detached membranes. **(b)** Axial T1-weighted MR image shows high signal intensity within the cyst, a finding consistent with hemorrhagic content. Bleeding into a hydatid cyst is an extremely rare complication and should be considered a less likely diagnosis.

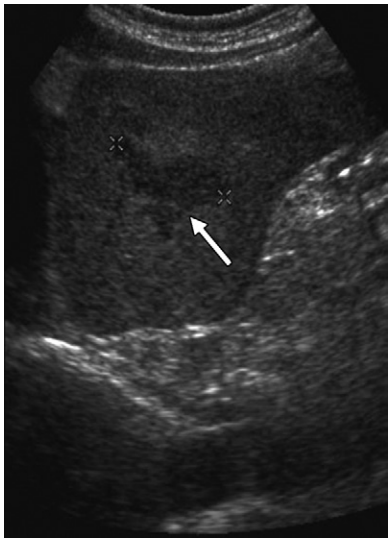

Figure 20. Hepatic fascioliasis in a 60-year-old man with fever, night sweats, and a history of watercress ingestion 3 months before admission. Sagittal US image of the left hepatic lobe shows ill-defined confluent hypoechoic nodules (between calipers; arrow) surrounded by mildly hyperechoic inflamed parenchyma. Laboratory examinations confirmed 60% eosinophilia, positive immunoglobulin G antibodies to *Fasciola,* and *Fasciola* eggs in the patient's stool.

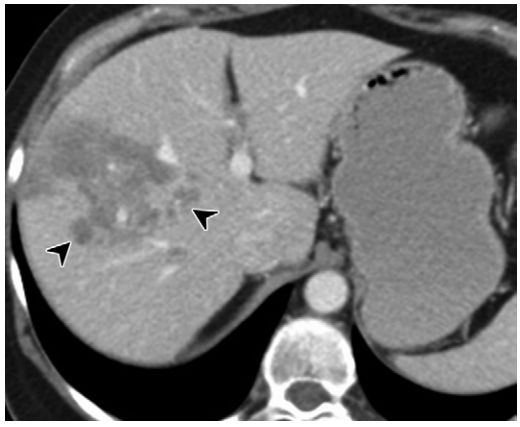

Figure 21. Fascioliasis in a 59-year-old woman who presented with right upper quadrant pain. Axial contrast-enhanced CT image shows a large area of segmental inflammation in the anterior right hepatic lobe, with multiple satellite microabscesses (arrowheads) that follow the course of the venous tracts.

Differential Diagnosis and Potential Pitfalls

Caroli Disease and Sclerosing Cholangitis.—Hepatobiliary fascioliasis may mimic Caroli disease and sclerosing cholangitis. Enhancing dots within periportal, nonenhancing, hypoattenuating nodules can appear similar to the "central dot sign" seen in Caroli disease (Fig 23). The linear periportal tracts of liver flukes may simulate findings of sclerosing cholangitis.

Neoplasms.—Intrahepatic cholangiocarcinoma, metastatic disease, and locally advanced gallbladder carcinoma may have a similar imaging appearance to that of hepatobiliary fascioliasis. However, linear tracts and, more importantly, eosinophilia should prompt consideration of possible fascioliasis.

Schistosomiasis

Trematode blood flukes of the genus *Schistosoma* cause schistosomiasis. Five species are responsible for human infections; *Schistosoma mansoni* and *Schistosoma japonicum* are the most common species affecting the liver (66). Schistosomiasis is endemic to tropical and subtropical areas of Africa, Asia, South America, and the Caribbean. Tourists to endemic areas are at risk for developing acute schistosomiasis, called Katayama disease, as well as chronic disease.

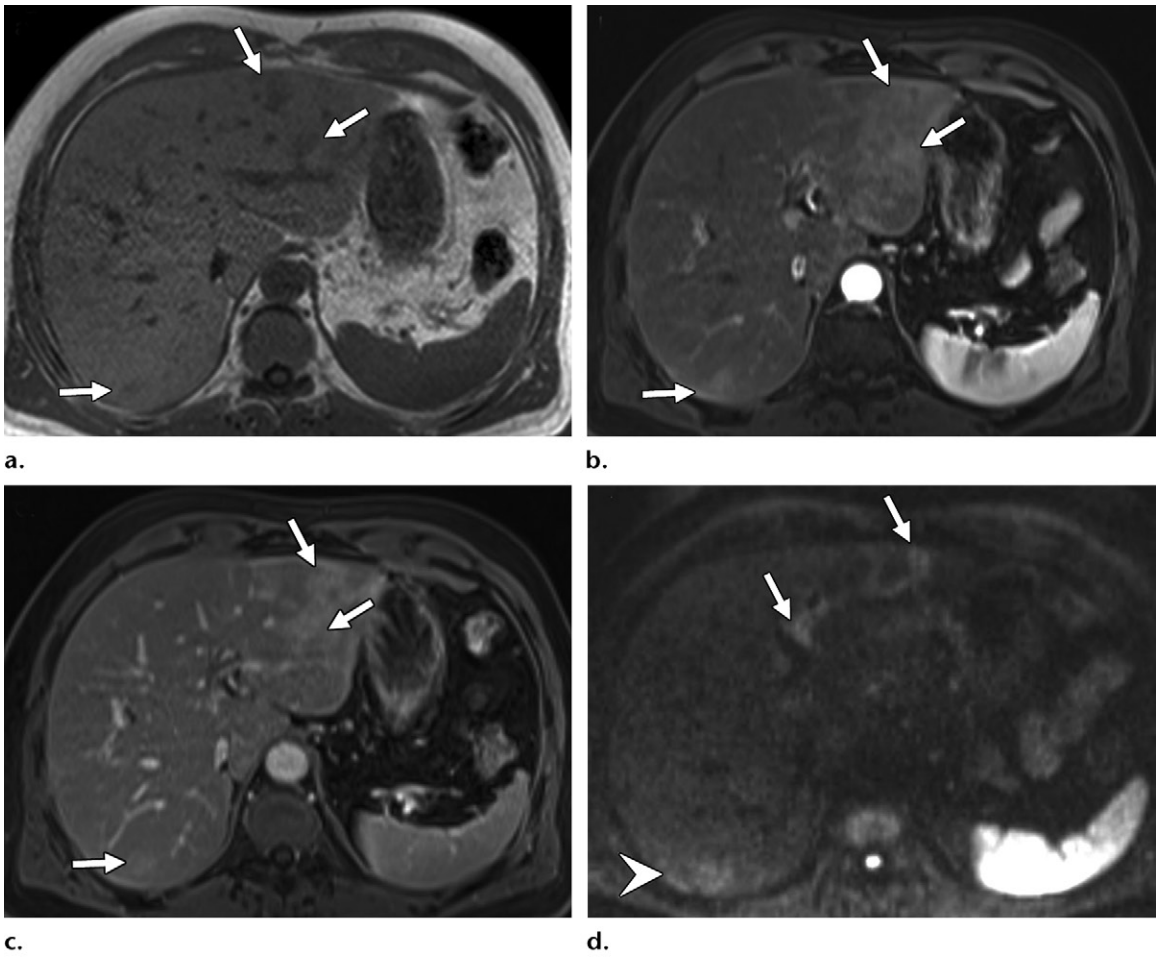

Figure 22. Hepatic fascioliasis in a 60-year-old man who presented with fever, night sweats, and a history of watercress ingestion 3 months before admission (same patient as in Fig 20). **(a)** Axial gradient-echo in-phase T1-weighted MR image shows hypointense ill-defined tracts in subcapsular areas of the left lateral and posterior right hepatic segments (arrows). **(b)** Axial contrast-enhanced arterial phase fat-suppressed T1-weighted MR image depicts early enhancement of the inflammatory tracts (arrows) and the surrounding hepatic parenchyma. **(c)** Axial contrast-enhanced delayed phase fat-suppressed T1-weighted MR image shows contrast agent retention in parasitic parenchymal tracts (arrows). **(d)** Axial diffusion-weighted image (b = 800 sec/mm^2) depicts restricted water diffusion in irregular ill-defined tracts in the subcapsular left hepatic lobe that course centrally toward the hilum (arrows). The second focus of subcapsular inflammation in the posterior segment (arrowhead) also shows water restriction. **(e)** Coronal T2-weighted MR image shows irregular hypointense linear filling defects in the distal bile duct (arrowhead), findings confirmed at endoscopy to be live parasites.

Schistosomes penetrate the human skin and migrate to their residence in the mesenteric veins. The eggs may be carried via the portal vein to the liver, where they lodge in the venules, causing granuloma formation, presinusoidal hypertension, and, with *S japonicum* infection, eventual calcifications (66).

The diagnosis is made on the basis of epidemiologic data, eosinophilia, the presence of living eggs in stool samples, or positive *Schistosoma* serologic findings. The first-line treatment of schistosomiasis is anthelminthic drugs such as praziquantel (66).

The imaging features of schistosomiasis are not seen until many years after initial infection, although hepatosplenomegaly and multiple small focal nodular lesions in the liver have been described in some acute cases (67). Changes of periportal fibrosis may be seen at US (11,68). The relatively larger eggs of *S mansoni* tend to lodge in the larger portal veins of the hilum; US

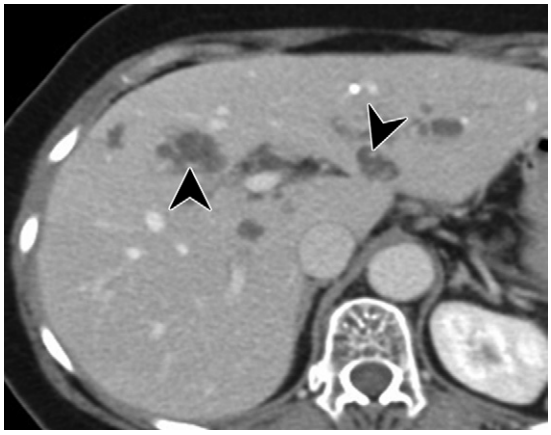

Figure 23. Hepatobiliary fascioliasis mimicking Caroli disease in a 62-year-old woman. Axial contrast-enhanced CT image shows enhancing dots (arrowheads) within periportal nonenhancing hypoattenuating nodules, findings that correspond to perivascular abscesses and result in a similar appearance to the "central dot sign" described in Caroli disease. Linear tracts, centripetal distribution, and blood eosinophilia should prompt consideration of hepatic fascioliasis. The diagnosis of fascioliasis was made after confirmation of parasite eggs in the patient's stool.

shows fibrous hyperechoic thick bands along the portal vein and its branches. A "bull's-eye" appearance has been reported in *S mansoni* infection and results from the anechoic portal vein surrounded by an echogenic mantle of fibrous tissue (11). The relatively smaller eggs of *S japonicum* are deposited along the smaller portal veins in the periphery of the liver; US shows hyperechoic polygonal septa mimicking a "fish scale" appearance (mosaic pattern) (68).

At CT, the classic pattern in *S japonicum* infection is the presence of calcified septa that usually are perpendicular to the liver capsule, giving the liver a "tortoise shell" or "turtle back" appearance (11,68). Other findings include low-attenuation periportal bands of fibrous septa spreading uniformly throughout the liver. At MR imaging, the septa are hypo- to isointense on T1-weighted images and hyperintense on T2-weighted images. The periportal fibrous bands show marked delayed enhancement after contrast agent administration (Fig 24b). Associated findings may include liver cirrhosis and signs of portal hypertension (68).

Differential Diagnosis and Potential Pitfalls

Autoimmune Hepatitis.—Distinguishing autoimmune hepatitis from schistosomiasis may be difficult on the basis of imaging findings alone. Similar fibrous septa within the liver parenchyma can be seen in both diseases (Fig 24). Epidemiologic, clinical, and laboratory findings (serum autoantibodies) are key to establishing an accurate diagnosis.

Clonorchiasis (Recurrent Pyogenic Cholangitis)

Clonorchiasis is caused by the liver fluke *Clonorchis sinensis* and is endemic in eastern Russia and Manchuria, South Korea, mainland China, Taiwan, and northern Vietnam (12,63). Humans are infected by ingesting the metacercariae in raw freshwater fish. The metacercariae ascend into the bile ducts to reside in the medium and small intrahepatic bile ducts, where they may lead to biliary obstruction, recurrent pyogenic cholangitis, biliary strictures, and cholangiocarcinoma. Parasite-induced mucin-secreting cells create bile with a high mucin content, which, when combined with adult flukes and eggs, serves as a nidus for bacterial superinfection and intrahepatic stone formation (12,69).

At US, clonorchiasis can manifest as diffuse mild to moderate dilatation of the small intrahepatic bile ducts and intraductal stones or sludge, with no or minimal dilatation of larger bile ducts and without an obstructing lesion (70). Occasionally, flukes or aggregates of eggs are shown as nonshadowing echogenic foci or casts within the bile ducts (12,70). CT and MR imaging findings simulate those at US—mild to moderate dilatation of the peripheral intrahepatic bile ducts without a focal obstructing lesion (12,71,72). Intrahepatic stones may also be seen (Fig 25). Periductal contrast enhancement may be detected if fibrosis has developed (12). The differential diagnoses include nonparasitic hepatolithiasis and sclerosing cholangitis. Sclerosing cholangitis differs from clonorchiasis by its more severe thickening of the bile ducts and discontinuous ductal dilatation (12,69).

The anthelminthic drug praziquantel is the treatment of choice (63). In patients with recurrent pyogenic cholangitis, antibiotics and endoscopic or surgical stone removal may be necessary.

Fungal Infections

Invasive fungal infection is a complication of prolonged neutropenia in patients with hematologic malignancies, in hematopoietic stem cell or solid-organ transplant recipients, and in other immunosuppressed patients (12,73). Although *Candida* species, *Aspergillus* species, and *Cryptococcus neoformans* account for 80% of all fungal infections, the spectrum of possible

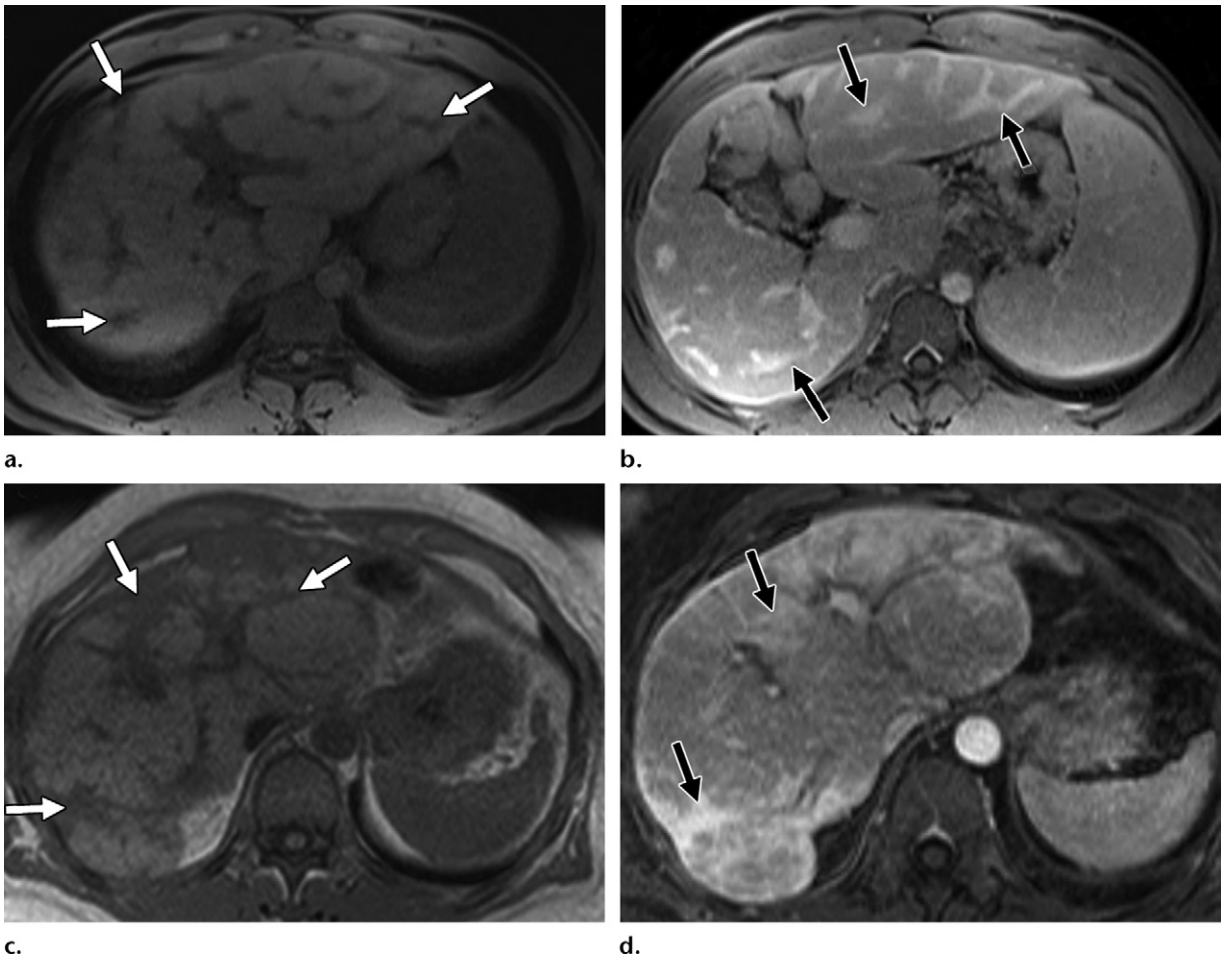

Figure 24. Schistosomiasis versus autoimmune hepatitis. **(a, b)** Schistosomiasis in a 42-year-old man. **(a)** Axial fat-suppressed T1-weighted MR image shows thick low-signal-intensity fibrous septa (arrows). **(b)** Axial contrast-enhanced fat-suppressed T1-weighted MR image shows enhancement of the subcapsular fibrous bands (arrows). **(c, d)** Autoimmune hepatitis in a 51-year-old woman. **(c)** Axial gradient-echo in-phase T1-weighted MR image shows subcapsular fibrosis with thick bands and confluent areas of low signal intensity (arrows). **(d)** Axial contrast-enhanced fat-suppressed T1-weighted MR image shows delayed enhancement of the thick bands and confluent areas of fibrosis (arrows), similar imaging features to those seen in the patient with schistosomiasis in **a** and **b**.

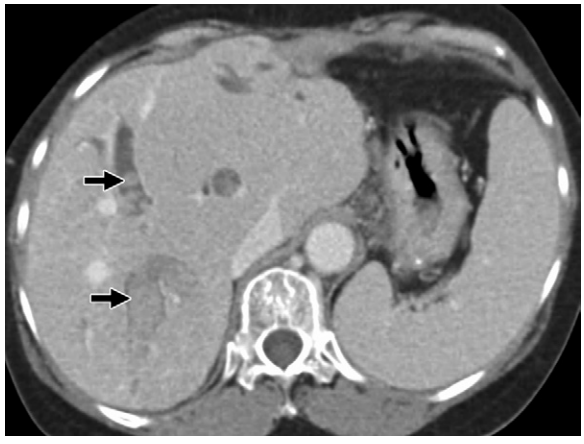

Figure 25. Clonorchiasis and recurrent pyogenic cholangitis in a 54-year-old woman who presented with fever and jaundice. Axial contrast-enhanced CT image shows moderate dilatation of the intrahepatic bile ducts without a focal obstructing lesion. Note the hyperattenuating intrahepatic stones and sludge (arrows).

opportunistic fungal pathogens also includes histoplasmosis, mucormycosis, and emerging pathogens such as yeasts, including *Trichosporon* and *Blastoschizomyces,* and hyaline hyphomycetes such as *Fusarium* (73).

Early recognition of hepatic fungal infection is crucial to initiate therapy and avoid fatal complications in these immunocompromised patients (74). However, imaging cannot be used to determine the specific underlying pathogen because many types of fungal diseases share similar characteristics at US, CT, and MR imaging (11).

Candidiasis

Hepatic candidiasis has been increasingly recognized as a manifestation of disseminated candidiasis in immunocompromised patients; imaging plays a critical role in prompt detection. The most

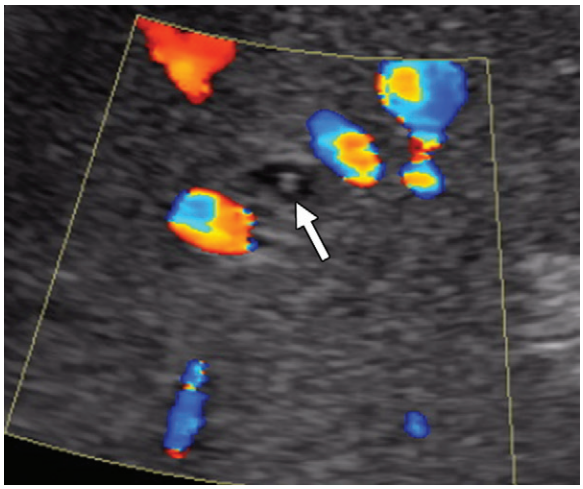

Figure 26. Hepatic candidiasis in a 63-year-old man with acute myelogenous leukemia who presented with fever. Color Doppler US image obtained during liver needle biopsy shows a hypoechoic well-defined lesion with a central hyperechoic nodule (arrow) and "bull's-eye" appearance. Subsequent cultures grew *Candida albicans.*

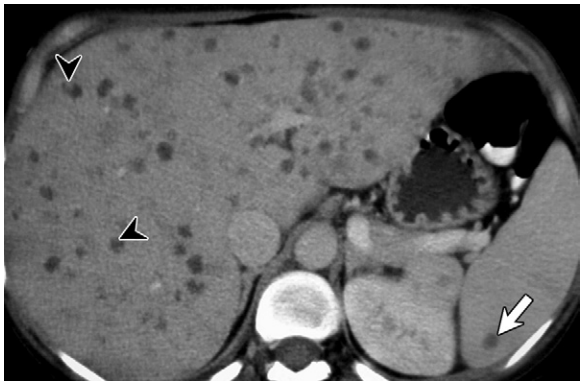

Figure 27. Disseminated candidiasis in a patient with neutropenia and acute myeloid leukemia. Axial contrast-enhanced CT image shows multiple hypoattenuating hepatic microabscesses. Tiny foci of increased attenuation (arrowheads) are seen in some of the abscesses, presumably representing pseudohyphae, a finding that helps distinguish these lesions from benign liver cysts. Note the splenic involvement (arrow).

common fungus to infect the liver and spleen is the *Candida* species (12,24). Patients usually present with fever unresponsive to standard antibiotics. Blood cultures, however, are positive in only 50% of cases (75). Therefore, confirmation often requires complementary studies, such as β-D-glucan detection (a cell wall constituent of *Candida* species and other fungi), a PCR test, or tissue sampling (75). Because the mortality rate in patients with invasive candidiasis is 30% despite antifungal therapy, early suspicion and detection are essential (74).

US features of hepatosplenic candidiasis have been summarized in four patterns (76): *(a)* "wheel-within-wheel" pattern, which consists of a hypoechoic nidus representing necrotic fungal debris, an inner hyperechoic ring composed of inflammatory cells, and a peripheral hypoechoic ring that represents fibrosis; *(b)* "bull's-eye" appearance, similar to the wheel-within-wheel pattern but lacking the hypoechoic nidus and consisting of only the inner hyperechoic inflammatory lesion and the outer hypoechoic ring of fibrosis (Fig 26); *(c)* hypoechoic nodule, which is the most common but least specific pattern and results from fibrosis in a region of prior inflammation; and *(d)* echogenic focus of scar or calcification with variable posterior acoustic shadowing. The last pattern occurs in later stages of infection and generally indicates early resolution (76).

CT usually reveals small low-attenuation hepatic and splenic lesions (Fig 27) (11,77). Occasionally, tiny foci with increased attenuation are detected in the center of the inflammatory nodules, presumably representing pseudohyphae, which helps to distinguish these lesions from benign liver cysts (78). In patients suspected of having hepatic fungal infection, arterial phase CT depicts significantly more hepatic lesions than does CT performed during other phases, and it shows more lesions with enhancement patterns of infection (77). As many as one-third of lesions may be hyperattenuating without central hypoattenuation in the arterial phase. Rim enhancement may also be detected (11,77).

MR imaging appears to be superior to CT and US for detection of fungal foci (11). In patients with persistent fever or failure of response to antibacterial antibiotics, MR imaging shows 100% sensitivity and 96% specificity for the diagnosis of hepatosplenic fungal disease (Fig 28) (79). Lesions appear minimally hypointense on T1-weighted images and markedly hyperintense on T2-weighted images. Depending on the degree of neutropenia recovery, intense ring enhancement can be seen on early gadolinium-enhanced arterial phase images (79). Fungal abscesses may also show restriction on diffusion-weighted images (21).

Histoplasmosis

Histoplasmosis is a common endemic fungal infection, especially in the Ohio, Missouri, and Mississippi River valleys of the United States (80). Hepatic involvement is seen in 90% of cases of disseminated histoplasmosis (80). Patients at risk for developing disseminated disease include patients with HIV infection and CD4 counts of less than 200 cells/μL, patients with primary immunodeficiency or other immunosuppressive disorders, and patients taking immunosuppressive medications. The diagnosis can be established with culture, antigen detection, or

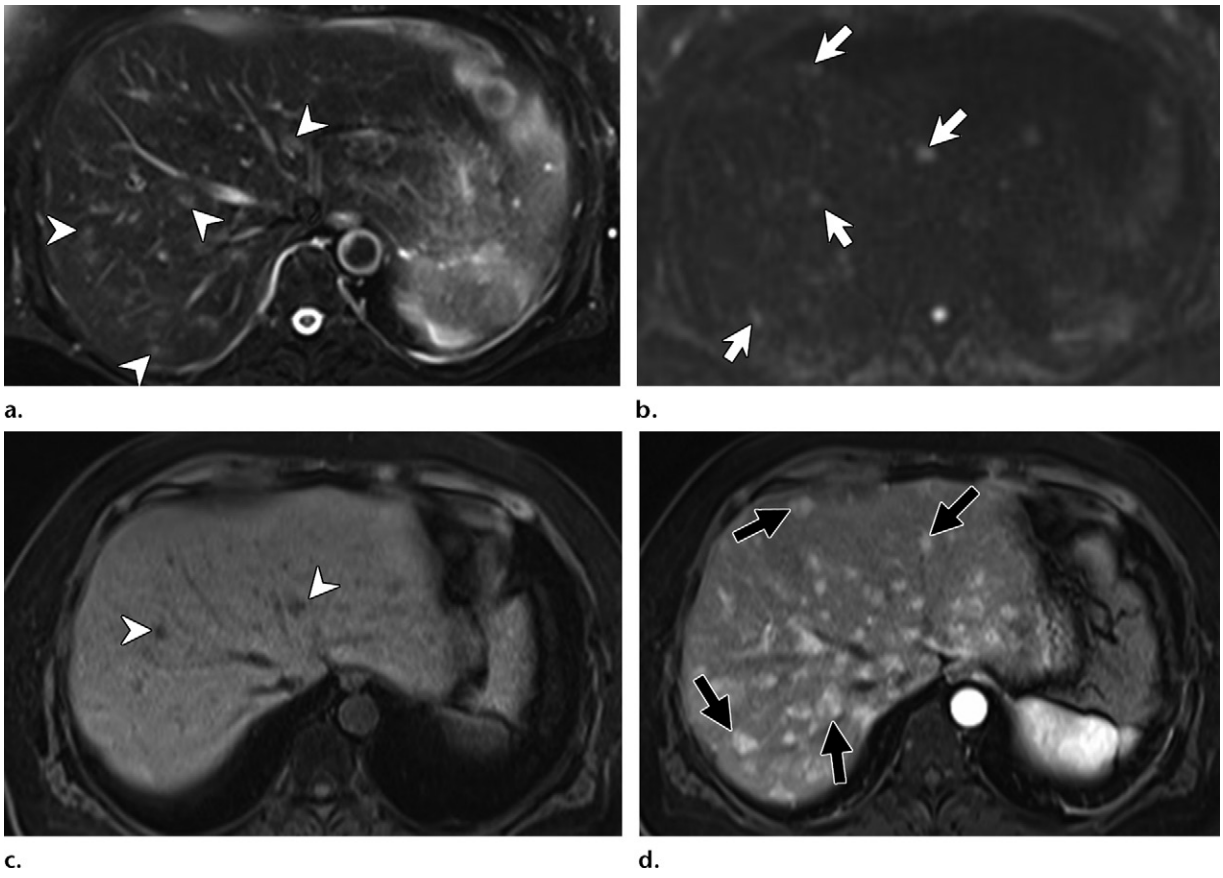

Figure 28. Disseminated candidiasis in a patient with neutropenia who presented with fever 34 days after a hematopoietic stem cell transplant. **(a)** Axial fat-suppressed T2-weighted MR image shows multiple small moderately hyperintense nodules scattered throughout the liver (arrowheads). **(b)** Axial diffusion-weighted image (b = 800 sec/mm^2) shows increased signal intensity of fungal foci (arrows) due to restricted water diffusion. **(c)** Axial fat-suppressed T1-weighted MR image depicts only some of the larger nodules as hypointense foci (arrowheads). **(d)** Axial contrast-enhanced arterial phase fat-suppressed T1-weighted MR image shows multiple ill-defined enhancing hepatic nodules (arrows). Arterial phase CT or MR images may depict more lesions at an earlier stage, especially before a necrotic central nidus develops.

antibody testing, but performance of these methods is not optimal, and histologic confirmation is often necessary (80).

Imaging findings of hepatic histoplasmosis are similar to those seen in candidiasis or other disseminated fungal diseases, with multiple small lesions seen throughout the liver parenchyma (11). The spleen is also almost invariably involved. Antifungal agents, including amphotericin B for severe cases and itraconazole for moderate disease, are used to treat hepatic histoplasmosis.

Differential Diagnosis and Potential Pitfalls.—The differential diagnosis of disseminated fungal disease with liver involvement includes other infections such as disseminated tuberculosis and hepatosplenic bartonellosis, lymphoma, leukemia, metastases, and sarcoidosis. Imaging findings alone may not help differentiate these entities. However, in patients with neutropenia, fungal disease must be considered to guide appropriate patient care.

Conclusion

The role of imaging is crucial in infectious liver diseases. Depending on the causative agent, imaging allows early disease detection, helps exclude other entities with similar clinical manifestations, and aids in definitive diagnosis, thus guiding appropriate patient care.

Although US findings are often nonspecific, CT and especially MR imaging findings together with clinical data can provide useful information to narrow the differential diagnosis, exclude neoplasm in challenging cases, and occasionally identify the underlying infectious agent (Fig 29). Furthermore, US and CT are important means to guide percutaneous aspiration or drainage when needed.

Familiarity with the epidemiology, pathogenesis, clinical manifestations, imaging features, and treatment of hepatic infections can aid in radiologic diagnosis and guide appropriate patient care. Cognizance of the potential pitfalls in image interpretation may help avoid unnecessary testing, procedures, and treatments.

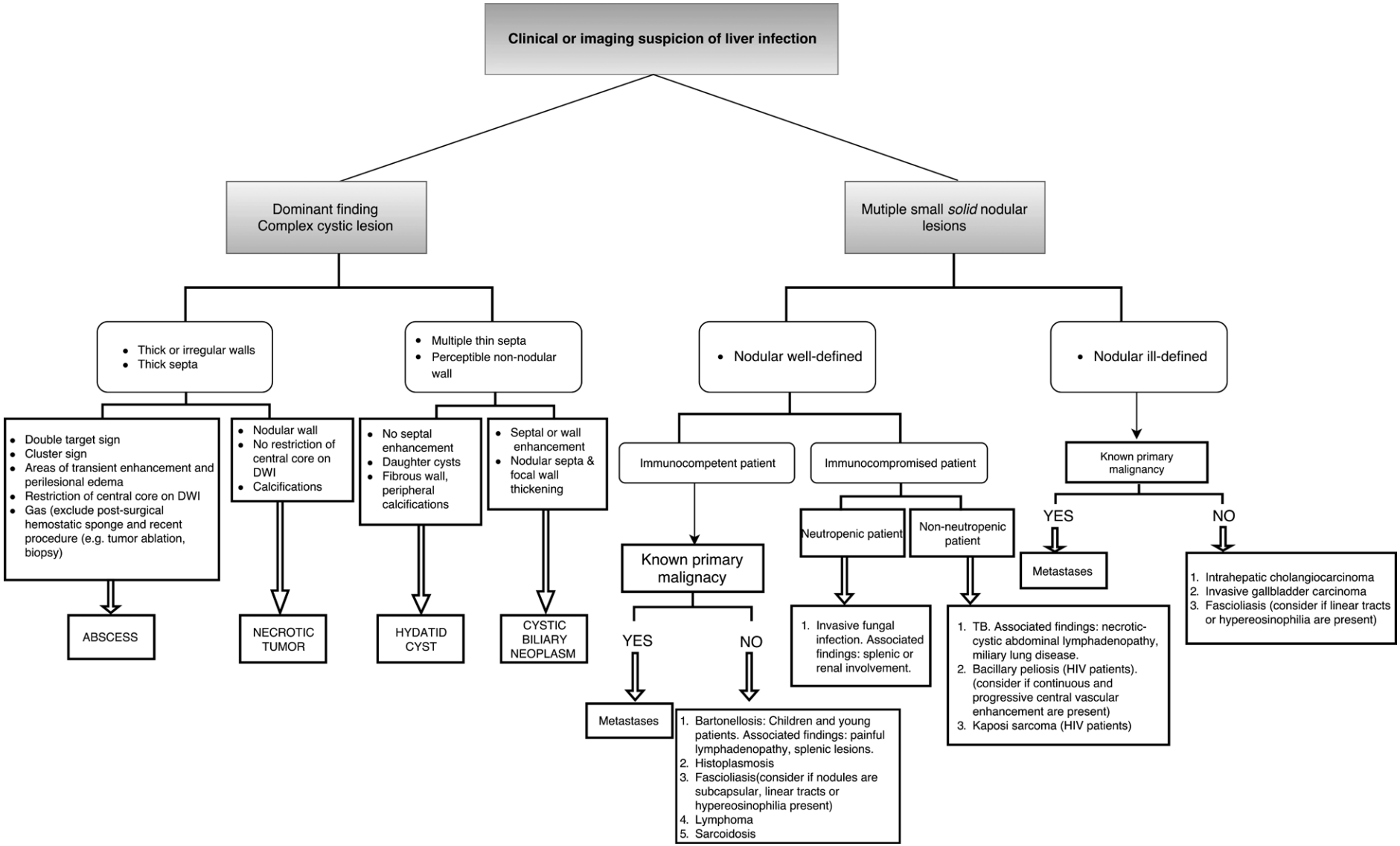

Figure 29. Flowchart shows differential diagnosis when there is clinical or imaging suspicion for infectious liver disease. *DWI* = diffusion-weighted images, *TB* = tuberculosis.

References

1. Wisplinghoff H, Appleton DL. Bacterial infections of the liver. In: Weber O, Protzer U, eds. Comparative hepatitis. Basel, Switzerland: Birkhäuser, 2008; 143–160.
2. Altemeier WA, Culbertson WR, Fullen WD, Shook CD. Intra-abdominal abscesses. Am J Surg 1973;125(1):70–79.
3. Mohsen AH, Green ST, Read RC, McKendrick MW. Liver abscess in adults: ten years experience in a UK centre. QJM 2002;95(12):797–802.
4. Rahimian J, Wilson T, Oram V, Holzman RS. Pyogenic liver abscess: recent trends in etiology and mortality. Clin Infect Dis 2004;39(11):1654–1659.
5. Huang CJ, Pitt HA, Lipsett PA, et al. Pyogenic hepatic abscess: changing trends over 42 years. Ann Surg 1996;223(5): 600–607; discussion 607–609.
6. Liu Y, Wang JY, Jiang W. An increasing prominent disease of *Klebsiella pneumoniae* liver abscess: etiology, diagnosis, and treatment. Gastroenterol Res Pract 2013;2013:258514.
7. Molton J, Phillips R, Gandhi M, et al. Oral versus intravenous antibiotics for patients with *Klebsiella pneumoniae* liver abscess: study protocol for a randomized controlled trial. Trials 2013;14(1):364.
8. Zerem E, Hadzic A. Sonographically guided percutaneous catheter drainage versus needle aspiration in the management of pyogenic liver abscess. AJR Am J Roentgenol 2007;189(3):W138–W142.
9. Halvorsen RA, Korobkin M, Foster WL, Silverman PM, Thompson WM. The variable CT appearance of hepatic abscesses. AJR Am J Roentgenol 1984;142(5):941–946.
10. Lin AC, Yeh DY, Hsu YH, et al. Diagnosis of pyogenic liver abscess by abdominal ultrasonography in the emergency department. Emerg Med J 2009;26(4):273–275.
11. Mortelé KJ, Segatto E, Ros PR. The infected liver: radiologic-pathologic correlation. RadioGraphics 2004;24(4): 937–955.
12. Benedetti NJ, Desser TS, Jeffrey RB. Imaging of hepatic infections. Ultrasound Q 2008;24(4):267–278.
13. Subramanyam BR, Balthazar EJ, Raghavendra BN, Horii SC, Hilton S, Naidich DP. Ultrasound analysis of solid-appearing abscesses. Radiology 1983;146(2):487–491.
14. Hui JY, Yang MK, Cho DH, et al. Pyogenic liver abscesses caused by *Klebsiella pneumoniae*: US appearance and aspiration findings. Radiology 2007;242(3):769–776.
15. Gabata T, Kadoya M, Matsui O, et al. Dynamic CT of hepatic abscesses: significance of transient segmental enhancement. AJR Am J Roentgenol 2001;176(3):675–679.
16. Jeffrey RB Jr, Tolentino CS, Chang FC, Federle MP. CT of small pyogenic hepatic abscesses: the cluster sign. AJR Am J Roentgenol 1988;151(3):487–489.
17. Mathieu D, Vasile N, Fagniez PL, Segui S, Grably D, Lardé D. Dynamic CT features of hepatic abscesses. Radiology 1985;154(3):749–752.
18. Alsaif HS, Venkatesh SK, Chan DS, Archuleta S. CT appearance of pyogenic liver abscesses caused by *Klebsiella pneumoniae*. Radiology 2011;260(1):129–138.
19. Balci NC, Semelka RC, Noone TC, et al. Pyogenic hepatic abscesses: MRI findings on T1- and T2-weighted and serial gadolinium-enhanced gradient-echo images. J Magn Reson Imaging 1999;9(2):285–290.
20. Méndez RJ, Schiebler ML, Outwater EK, Kressel HY. Hepatic abscesses: MR imaging findings. Radiology 1994;190 (2):431–436.
21. Chan JH, Tsui EY, Luk SH, et al. Diffusion-weighted MR imaging of the liver: distinguishing hepatic abscess from cystic or necrotic tumor. Abdom Imaging 2001;26(2): 161–165.
22. Lee TY, Wan YL, Tsai CC. Gas-containing liver abscess: radiological findings and clinical significance. Abdom Imaging 1994;19(1):47–52.
23. Oei T, vanSonnenberg E, Shankar S, Morrison PR, Tuncali K, Silverman SG. Radiofrequency ablation of liver tumors: a new cause of benign portal venous gas. Radiology 2005;237(2):709–717.
24. Doyle DJ, Hanbidge AE, O'Malley ME. Imaging of hepatic infections. Clin Radiol 2006;61(9):737–748.
25. Kim SB, Je BK, Lee KY, Lee SH, Chung HH, Cha SH. Computed tomographic differences of pyogenic liver abscesses caused by *Klebsiella pneumoniae* and non-*Klebsiella pneumoniae*. J Comput Assist Tomogr 2007;31(1):59–65.
26. Kim YK, Kim CS, Lee JM, Ko SW, Moon WS, Yu HC. Solid organizing hepatic abscesses mimic hepatic tumor: multiphasic computed tomography and magnetic resonance imaging findings with histopathologic correlation. J Comput Assist Tomogr 2006;30(2):189–196.
27. Holzapfel K, Rummeny E, Gaa J. Diffusion-weighted MR imaging of hepatic abscesses: possibility of different apparent diffusion coefficient (ADC)–values in early and mature abscess formation. Abdom Imaging 2007;32(4):538–539.
28. Baron RL, Campbell WL, Dodd GD 3rd. Peribiliary cysts associated with severe liver disease: imaging-pathologic correlation. AJR Am J Roentgenol 1994;162(3):631–636.
29. Semelka RC, Hussain SM, Marcos HB, Woosley JT. Biliary hamartomas: solitary and multiple lesions shown on current MR techniques including gadolinium enhancement. J Magn Reson Imaging 1999;10(2):196–201.
30. Young ST, Paulson EK, McCann RL, Baker ME. Appearance of oxidized cellulose (Surgicel) on postoperative CT scans: similarity to postoperative abscess. AJR Am J Roentgenol 1993;160(2):275–277.
31. Arnold AC, Sodickson A. Postoperative Surgicel mimicking abscesses following cholecystectomy and liver biopsy. Emerg Radiol 2008;15(3):183–185.
32. World Health Organization. Global tuberculosis report 2014. Geneva, Switzerland: World Health Organization, 2014; 1–118.
33. Burrill J, Williams CJ, Bain G, Conder G, Hine AL, Misra RR. Tuberculosis: a radiologic review. RadioGraphics 2007;27(5):1255–1273.
34. Jadvar H, Mindelzun RE, Olcott EW, Levitt DB. Still the great mimicker: abdominal tuberculosis. AJR Am J Roentgenol 1997;168(6):1455–1460.
35. Yu RS, Zhang SZ, Wu JJ, Li RF. Imaging diagnosis of 12 patients with hepatic tuberculosis. World J Gastroenterol 2004;10(11):1639–1642.
36. Kawamori Y, Matsui O, Kitagawa K, Kadoya M, Takashima T, Yamahana T. Macronodular tuberculoma of the liver: CT and MR findings. AJR Am J Roentgenol 1992;158(2):311–313.
37. Klotz SA, Ianas V, Elliott SP. Cat-scratch disease. Am Fam Physician 2011;83(2):152–155.
38. Florin TA, Zaoutis TE, Zaoutis LB. Beyond cat scratch disease: widening spectrum of *Bartonella henselae* infection. Pediatrics 2008;121(5):e1413–e1425.
39. Carithers HA. Cat-scratch disease: an overview based on a study of 1200 patients. Am J Dis Child 1985;139(11): 1124–1133.
40. Hopkins KL, Simoneaux SF, Patrick LE, Wyly JB, Dalton MJ, Snitzer JA. Imaging manifestations of cat-scratch disease. AJR Am J Roentgenol 1996;166(2):435–438.
41. Danon O, Duval-Arnould M, Osman Z, et al. Hepatic and splenic involvement in cat-scratch disease: imaging features. Abdom Imaging 2000;25(2):182–183.
42. Iannaccone R, Federle MP, Brancatelli G, et al. Peliosis hepatis: spectrum of imaging findings. AJR Am J Roentgenol 2006;187(1):W43–W52.
43. Torabi M, Hosseinzadeh K, Federle MP. CT of nonneoplastic hepatic vascular and perfusion disorders. RadioGraphics 2008;28(7):1967–1982.
44. Ryder SD, Beckingham IJ. ABC of diseases of liver, pancreas, and biliary system: acute hepatitis. BMJ 2001;322 (7279):151–153.
45. Kurtz AB, Rubin CS, Cooper HS, et al. Ultrasound findings in hepatitis. Radiology 1980;136(3):717–723.
46. Ahn JH, Chung JJ, Yu JS, Kim JH, Cho ES, Kim DJ. Prognostic value of gallbladder wall thickening in patients with acute hepatitis A. Ultrasonography 2015;34(2):139–143.
47. Fabre A, Couvelard A, Degott C, et al. Dengue virus induced hepatitis with chronic calcific changes. Gut 2001;49(6): 864–865.
48. Stanley SL Jr. Amoebiasis. Lancet 2003;361(9362): 1025–1034.
49. Ralls PW, Quinn MF, Boswell WD Jr, Colletti PM, Radin DR, Halls J. Patterns of resolution in successfully treated hepatic amebic abscess: sonographic evaluation. Radiology 1983;149(2):541–543.

50. Radin DR, Ralls PW, Colletti PM, Halls JM. CT of amebic liver abscess. AJR Am J Roentgenol 1988;150(6):1297–1301.
51. Landay MJ, Setiawan H, Hirsch G, Christensen EE, Conrad MR. Hepatic and thoracic amaebiasis. AJR Am J Roentgenol 1980;135(3):449–454.
52. Elizondo G, Weissleder R, Stark DD, et al. Amebic liver abscess: diagnosis and treatment evaluation with MR imaging. Radiology 1987;165(3):795–800.
53. Eckert J, Gemmell MA, Meslin FX, Pawloski ZS, eds. WHO/OIE manual on echinococcosis in humans and animals: a public health problem of global concern. Paris, France: World Organisation for Animal Health, 2001.
54. Pedrosa I, Saíz A, Arrazola J, Ferreirós J, Pedrosa CS. Hydatid disease: radiologic and pathologic features and complications. RadioGraphics 2000;20(3):795–817.
55. Marani SA, Canossi GC, Nicoli FA, Alberti GP, Monni SG, Casolo PM. Hydatid disease: MR imaging study. Radiology 1990;175(3):701–706.
56. Levy AD, Murakata LA, Abbott RM, Rohrmann CA Jr. Benign tumors and tumorlike lesions of the gallbladder and extrahepatic bile ducts: radiologic-pathologic correlation. RadioGraphics 2002;22(2):387–413.
57. Martin DR, Kalb B, Sarmiento JM, Heffron TG, Coban I, Adsay NV. Giant and complicated variants of cystic bile duct hamartomas of the liver: MRI findings and pathological correlations. J Magn Reson Imaging 2010;31(4):903–911.
58. Firmin A, Bernadette N, Catherine M, et al. Intracystic bleeding of a solitary hydatid cyst: a rare complication of a rare disease in central Africa—a case report. Case Rep Clin Med 2013;2(2):163–166.
59. Haddad MC, Birjawi GA, Khouzami RA, Khoury NJ, El-Zein YR, Al-Kutoubi AO. Unilocular hepatic echinococcal cysts: sonography and computed tomography findings. Clin Radiol 2001;56(9):746–750.
60. Mas-Coma S, Bargues MD, Valero MA. Fascioliasis and other plant-borne trematode zoonoses. Int J Parasitol 2005;35(11-12):1255–1278.
61. Behm CA, Sangster NC. Pathology, pathophysiology and clinical aspects. In: Dalton JP, ed. Fasciolosis. Wallingford, England: CAB International, 1999; 185–224.
62. Kabaalioglu A, Ceken K, Alimoglu E, et al. Hepatobiliary fascioliasis: sonographic and CT findings in 87 patients during the initial phase and long-term follow-up. AJR Am J Roentgenol 2007;189(4):824–828.
63. World Health Organization. Report of the WHO Expert Consultation on Foodborne Trematode Infections and Taeniasis/Cysticercosis. Geneva, Switzerland: World Health Organization, 2011.
64. Leon M, Alave J, Alvarado R, Gotuzzo E, Terashima A, Seas C. A 52-year-old woman with a subcapsular liver hematoma. Clin Infect Dis 2011;52(9):1137, 1195–1196.
65. Cevikol C, Karaali K, Senol U, et al. Human fascioliasis: MR imaging findings of hepatic lesions. Eur Radiol 2003;13(1):141–148.
66. Bica I, Hamer DH, Stadecker MJ. Hepatic schistosomiasis. Infect Dis Clin North Am 2000;14(3):583–604, viii.
67. Passos MC, Silva LC, Ferrari TC, Faria LC. Ultrasound and CT findings in hepatic and pancreatic parenchyma in acute schistosomiasis. Br J Radiol 2009;82(979):e145–e147.
68. Manzella A, Ohtomo K, Monzawa S, Lim JH. Schistosomiasis of the liver. Abdom Imaging 2008;33(2):144–150.
69. Choi BI, Han JK, Hong ST, Lee KH. Clonorchiasis and cholangiocarcinoma: etiologic relationship and imaging diagnosis. Clin Microbiol Rev 2004;17(3):540–552.
70. Lim JH, Ko YT, Lee DH, Kim SY. Clonorchiasis: sonographic findings in 59 proved cases. AJR Am J Roentgenol 1989;152(4):761–764.
71. Choi BI, Kim HJ, Han MC, Do YS, Han MH, Lee SH. CT findings of clonorchiasis. AJR Am J Roentgenol 1989;152(2):281–284.
72. Jeong YY, Kang HK, Kim JW, Yoon W, Chung TW, Ko SW. MR imaging findings of clonorchiasis. Korean J Radiol 2004;5(1):25–30.
73. Alexander BD, Pfaller MA. Contemporary tools for the diagnosis and management of invasive mycoses. Clin Infect Dis 2006;43(suppl 1):S15–S27.
74. Andes DR, Safdar N, Baddley JW, et al. Impact of treatment strategy on outcomes in patients with candidemia and other forms of invasive candidiasis: a patient-level quantitative review of randomized trials. Clin Infect Dis 2012;54(8):1110–1122.
75. Clancy CJ, Nguyen MH. Finding the "missing 50%" of invasive candidiasis: how nonculture diagnostics will improve understanding of disease spectrum and transform patient care. Clin Infect Dis 2013;56(9):1284–1292.
76. Pastakia B, Shawker TH, Thaler M, O'Leary T, Pizzo PA. Hepatosplenic candidiasis: wheels within wheels. Radiology 1988;166(2):417–421.
77. Metser U, Haider MA, Dill-Macky M, Atri M, Lockwood G, Minden M. Fungal liver infection in immunocompromised patients: depiction with multiphasic contrast-enhanced helical CT. Radiology 2005;235(1):97–105.
78. Moore NJ, Leef JL 3rd, Pang Y. Systemic candidiasis. RadioGraphics 2003;23(5):1287–1290.
79. Semelka RC, Kelekis NL, Sallah S, Worawattanakul S, Ascher SM. Hepatosplenic fungal disease: diagnostic accuracy and spectrum of appearances on MR imaging. AJR Am J Roentgenol 1997;169(5):1311–1316.
80. Lamps LW, Molina CP, West AB, Haggitt RC, Scott MA. The pathologic spectrum of gastrointestinal and hepatic histoplasmosis. Am J Clin Pathol 2000;113(1):64–72.